Title

Differential effects of nitrate, ammonium, and urea as N sources for microbial communities in the North Pacific Ocean

Journal

Limnology and Oceanography, 62(6)

ISSN

0024-3590

Authors

Shilova, IN
Mills, MM
Robidart, JC
et al.

Publication Date

2017-11-01

DOI

10.1002/lno.10590

Peer reviewed

Title

Differential effects of nitrate, ammonium and urea as N sources for microbial communities in the North Pacific Ocean

Authors

[1]Shilova IN[a], [2]Mills MM[a], [3]Robidart JC, [1]Turk-Kubo KA, [4]Björkman KM, [1]Kolber Z, [5]Rapp I., [2]van Dijken GL, [4]Church MJ[†], [2]Arrigo KR, [5]Achterberg EP, [1]Zehr JP*

[1]University of California Santa Cruz, CA, USA; [2]Stanford University, Stanford, CA, USA; [3]National Oceanography Centre, Southampton, UK; [4]University of Hawaii at Manoa, Honolulu, HI, USA; [5]GEOMAR Helmholtz Centre for Ocean Research, Kiel, Germany

[a]Equal contribution

[†] Present address: Flathead Lake Biological Station, University of Montana, Polson, MT, USA

*Correspondence: Department of Ocean Sciences, University of California Santa Cruz, 1156 High Street, Santa Cruz, CA 95064; Email: zehrj@ucsc.edu

Running title: N effects on microbial communities

Keywords: nitrogen, phytoplankton, microbial community, *Prochlorococcus*, *Synechococcus*, urea, nitrate, ammonium, iron, nutrient limitation, North Pacific, oligotyping

Abstract

Nitrogen (N) is the major limiting nutrient for phytoplankton growth and productivity in large parts of the world's oceans. Differential preferences for specific N substrates may be important in controlling phytoplankton community composition. To date, there is limited information on how specific N substrates influence the composition of naturally occurring microbial communities. We investigated the effect of nitrate (NO_3^-), ammonium (NH_4^+) and urea on microbial and phytoplankton community composition (cell abundances and 16S rRNA gene profiling) and functioning (photosynthetic activity, carbon fixation rates) in the oligotrophic waters of the North Pacific Ocean. All N substrates tested significantly stimulated phytoplankton growth and productivity. Urea resulted in the greatest (>300%) increases in chlorophyll *a* (<0.06 and ~0.19 μg L^{-1} in the control and urea addition, respectively) and productivity (<0.4 and ~1.4 μmol C L^{-1} d^{-1} in the control and urea addition, respectively) at two experimental stations, largely due to increased abundances of *Prochlorococcus* (Cyanobacteria). Two abundant clades of *Prochlorococcus*, High Light I and II, demonstrated similar responses to urea, suggesting this substrate is likely an important N source for natural *Prochlorococcus* populations. In contrast, the heterotrophic community composition changed most in response to NH_4^+. Finally, the time and magnitude of response to N amendments varied with geographic location, likely due to differences in microbial community composition and their nutrient status. Our results provide support for the hypothesis that changes in N supply would likely favor specific populations of phytoplankton in different oceanic regions and thus, affect both biogeochemical cycles and ecological processes.

Introduction

Nitrogen (N) is a major component of cell constituents, including proteins and nucleic acids, and is considered the primary limiting element for phytoplankton growth and photosynthetic carbon fixation in oligotrophic oceans (Eppley et al. 1977; Graziano et al. 1996; Mills et al. 2004; Moore et al. 2013). While there is an intricate balance among iron (Fe), phosphorus (P) and N in shaping microbial communities in the marine environment, nutrient enrichment experiments have demonstrated that the availability of N alone can stimulate growth of phytoplankton and affect heterotrophic communities in the oligotrophic ocean (Mills et al. 2004, 2008; Bonnet et al. 2008; Davey et al. 2008; Moore et al. 2008; Ortega-Retuerta et al. 2012).

N actively cycles in the upper ocean where sunlight provides energy that rapidly fuels production and consumption of N compounds. The major forms of N in the surface ocean include dinitrogen gas (N_2), ammonium (NH_4^+), nitrate (NO_3^-), nitrite (NO_2^-) and dissolved organic N (DON). N_2 fixation can account for 40-50% of net community production in the North Pacific Subtropical Gyre (NPSG) (Böttjer et al. 2016), however, net community production in this ecosystem is less than 10% of gross primary production (Quay et al. 2010). Although abundant, the bulk of the DON pool, except urea, amino acids and nucleotides, generally do not appear readily bioavailable and are believed to be minor sources of N for most phytoplankton (Aluwihare and Meador 2008; Mulholland and Lomas 2008). The major fixed N sources (NH_4^+, NO_3^-, and urea) have different sources and rates of production and turnover. Regeneration by heterotrophic bacteria, and excretion and release by zooplankton, are the major natural sources of NH_4^+ and urea in the upper ocean (Corner and Newell 1967; Mayzaud et al. 1973; Mitamura and Saijo 1981; Bidigare 1983; Hansell and Goering 1989; Bronk et al. 1998). Regenerated

70 production supported by this rapidly recycled N accounts for over 90% of gross primary
71 production in the oligotrophic oceans (Eppley and Peterson 1979). NO_3^- is supplied to the
72 euphotic zone predominately via mixing or upwelling of sub-euphotic zone waters with
73 additional contributions derived from nitrification within the euphotic zone (Dore and Karl 1996;
74 Yool et al. 2007) and atmospheric deposition (Duce et al. 2008). N from sources external to the
75 surface ocean supports "new" production, which balances N export losses due to sinking to the
76 deep ocean (Dugdale and Goering 1967). New N is also introduced through N_2 fixation carried
77 out by diazotrophs, a small subset of the marine microbial community (Dugdale and Goering
78 1967; Zehr and Kudela 2011). Recycling of diazotroph organic matter transfers this new N to the
79 dissolved pool as DON (e.g. amino acids and urea) and/or NH_4^+ where it can be used to fuel
80 primary production (Montoya et al. 2002; Zehr and Kudela 2011). Thus, the chemical form of N
81 is an important factor in the functioning of ocean ecosystems.
82 Microbial communities that utilize dissolved N in oligotrophic oceans are diverse, but are
83 comprised largely of cyanobacteria (*Prochlorococcus* and *Synechococcus*), diatoms, eukaryotic
84 picoplankton (for example, prymnesiophytes and pelagophytes) and a variety of heterotrophic
85 bacteria (including *Pelagibacter ubique*) and Archaea (Waterbury et al. 1979; Chisholm et al.
86 1988; DuRand et al. 2001; Karner et al. 2001; Morris et al. 2002; Worden et al. 2004). These
87 microorganisms have a variety of N assimilation strategies that differ in the rates of N uptake and
88 assimilation, regulation of N metabolism, and their abilities to use different N forms. For
89 example, N-limited Low Light (LL) *Prochlorococcus* strains appear unable to grow on NO_3^-
90 (Moore et al. 2002), while some strains of the High Light (HL) ecotypes are able to assimilate
91 NO_3^-, although at reduced rates of growth relative to other substrates (e.g. NH_4^+, Martiny et al.
92 2009; Berube et al. 2015). Many marine microorganisms use NO_3^- as a source of N, including

93 diatoms and *Synechococcus*, as well as some heterotrophic bacteria (Allen et al. 2001, 2006;
94 Casey et al. 2007; Collier et al. 2012). Isotopic analyses suggest that eukaryotic phytoplankton
95 smaller than 30 μm in the Sargasso Sea acquire a major fraction of their N demand from NO_3^-
96 (Fawcett et al. 2011). The assimilation of urea by phototrophic and heterotrophic marine
97 microorganisms is common across numerous phylogenetic groups and ecological niches
98 (McCarthy et al. 1972a, b; Hallam et al. 2006; Baker et al. 2009; Collier et al. 2009; review by
99 Solomon et al. 2010). Many *Prochlorococcus* strains and all tested *Synechococcus* strains can
100 utilize urea, yet this N substrate supports different growth rates within each genus (Moore et al.
101 2002). Moreover, rates of urea uptake and assimilation in natural microbial populations appear
102 comparable to those of NH_4^+ (Sahlsten 1987; Price and Harrison 1988), although rates differ
103 among phytoplankton taxa (Lomas and Glibert, 2000; Moore et al. 2002; Fan et al. 2003).
104 Despite the accumulated knowledge about N utilization by marine microorganisms, taxon-
105 specific preferences and utilization efficiencies for different N species is still ambiguous,
106 especially in the oligotrophic open ocean.
107 The form and supply of different N substrates are important controls on microbial
108 community composition. Understanding the effect of different N forms is critical because N
109 supply to the surface oceans will likely change due to greater stratification caused by climate
110 change (Gruber and Galloway 2008; Capotondi et al. 2012; Kim et al. 2014), and the projected
111 increase in atmospheric anthropogenic N deposition (Duce et al. 2008). We performed nutrient
112 enrichment experiments to determine the functional and taxonomic responses in microbial
113 communities to different N forms and whether the response varies depending on the nutrient
114 status (mesotrophic versus oligotrophic) in the North Pacific Ocean. The measured functional
115 responses included CO_2 fixation rates and changes in chlorophyll *a* (Chl *a*) and photosynthetic

parameters, while the taxonomic responses were assessed by quantifying the abundance of major phytoplankton groups and heterotrophic bacteria as well as assessing relative shifts in cyanobacterial and heterotrophic community composition based on 16S rRNA gene sequencing.

Materials and Methods

Nutrient amendments experiments

Experiments were conducted in August of 2014 during the Nitrogen Effects on Marine microOrganisms cruise (NEMO, R/V *New Horizon*) at two sites in the North Pacific Ocean: one within the western part of transitional zone of California Current System (CCS; Station 38, hereafter referred to as TZ), and one in the oligotrophic NPSG (Station 52, hereafter referred to as GY: Fig. 1). The TZ site was in an anticyclonic eddy, based on the sea surface height anomaly (Fig. 1b). The two sites were chosen based on a priori assumptions of nutrient limitation of primary productivity at each site. The availability of Fe can play an important role in controlling phytoplankton growth in the CCS (Biller and Bruland 2014). In contrast, N was assumed to be limiting primary productivity in the NPSG. All experiments were undertaken using strict trace-metal clean techniques (Mills et al. 2004) during the preparation and sampling of the experiments. Water at each station was collected from 25 m depth using a towed fish with Teflon diaphragm pump. The water was pumped gently into a 40 L carboy in a trace-metal clean laboratory van. This allowed mixing of the seawater before it was distributed into incubation bottles. Seawater was subsampled into 4 L polycarbonate bottles (Thermo Scientific™ Nalgene™) that had been acid-washed and, prior to the experiment, rinsed thoroughly with seawater at the site of each experiment. The bottles used in the first experiment were acid-rinsed and reused for the same treatments in the second experiment. In the TZ site experiment, triplicate

incubation bottles were amended with either NO_3^- (final concentration 5.0 μmol L^{-1}), NH_4^+ (final concentration 5.0 μmol L^{-1}), urea (final concentration 5.0 μmol N L^{-1}), 0.2 μm pre-filtered deep (600 m) seawater (FDW) (12.5% of total volume, equivalent to ~5 μmol L^{-1} NO_3^- addition), Fe^{3+}(final concentration 2 nmol L^{-1}) or a combined treatment containing NO_3^- and Fe^{3+} (final concentrations of 5 μmol L^{-1} and 2 nmol L^{-1}, respectively). The Fe and Fe+NO_3^- treatments were used to test for Fe and Fe+NO_3^- co-limitation. The GY experiment was similar in design with the exception that all N compounds were added to achieve a final concentration of 2.5 μmol N L^{-1}, and 6% of total volume of FDW was added (an approximately 2.5 μmol L^{-1} NO_3^- addition). The N additions in the TZ experiment were higher than in the GY experiment based on previous work in the CCS by Biller and Bruland (2014) who measured residual NO_3^- concentrations in the transitional zone of CCS ranging from 5-15 μmol L^{-1}, while residual NO_3^- at the GY was negligible (<10 nmol L^{-1}). In both experiments, the Controls consisted of triplicate bottles filled with unamended seawater from the respective station and depth. The Controls were incubated and processed in the same manner as the experimental treatments. All nutrient additions were undertaken in a laminar flow hood. The nutrient solutions, except the Fe solution, were passed through Chelex100 to minimize trace metal contamination. Purity controls were measured for all stocks to ensure the absence of contamination (i.e., Fe stocks did not contain dissolved N, N stocks did not contain Fe, and individual N stocks were not contaminated with other N species). Incubation bottles were placed in a flow-through surface seawater incubator, to achieve surface ocean temperatures during the experiment, with neutral screening to attenuate incident light to approximately 35% of the surface solar irradiance. The setup and samplings of the setup (T0), and at 24 (T24) and 48 (T48) hrs after the start of the incubation were undertaken before dawn. Rates of primary productivity and concentrations of Chl *a* and nutrients were measured in

samples immediately after the nutrient amendments (T0) and at T48. Samples for photophysiological parameters, cell abundance, and microbial community composition were collected prior to the nutrient amendments (T0), at T24, and T48.

Nutrient analysis

Samples for subsequent analyses of nutrient concentrations were collected in acid-washed, sample rinsed polyethylene bottles and stored frozen at -20°C until analyzed (Dore et al. 1996). NO_3^-+NO_2^-, soluble reactive phosphorus (SRP) and $Si(OH)_4$ concentrations (µmol L^{-1}) were determined using a segmented flow continuous flow automated nutrient analyzer (SEAL Analytical - AA3) using standard colorimetric techniques (Strickland and Parson, 1972). Accuracy of each analysis was checked using WAKO the International Cooperative Study of the Kuroshio and Adjacent Regions (CSK) and Ocean Scientific International Ltd. (OSIL) reference materials. NO_3^-+NO_2^- concentrations <500 nmol L^{-1} were determined using the high-sensitivity chemiluminescence technique (Garside 1982; Dore and Karl 1996) with a detection limit of 1 nmol L^{-1}. NH_4^+ samples were measured using the SEAL AA3 coupled with a 2 m liquid waveguide capillary cell, employing indophenol blue chemistry (Li et al. 2005; Zhu et al. 2014). The limit of detection for this method is 4 nmol L^{-1}.

Samples for subsequent analyses of trace metal concentrations were collected using an acid-cleaned hose (polyvinyl chloride, PVC) attached to a plastic-coated steel cable and lowered to the desired collection depth (25 m). Water was pumped to the surface using a Teflon bellows pump (Almatec A15) and transferred, entirely enclosed, into a trace-metal clean sampling container located in an on-deck trace-metal clean lab. Samples for the determination of dissolved Fe concentrations were filtered through a 0.2 µm Sartobran 300 capsule filter (Sartobran 300,

185 Sartorius), collected in acid-cleaned 125 mL low density polyethylene (LDPE, Nalgene) bottles,
186 and immediately acidified with 150 µL hydrochloric acid (~11 mol L^{-1} HCl, OPTIMA grade,
187 Fisher Scientific) to a final pH of 1.9. Dissolved Fe samples from the incubation experiments
188 were collected at T0 and T48. The samples were filtered using 0.45 µm polycarbonate membrane
189 filters (Millipore) mounted in an acid cleaned filter holder (Swinnex, Millipore), acidified to pH
190 1.9. and analyzed on-board ship using flow injection analysis (FIA). Dissolved Fe was
191 determined on-board the ship using luminol chemiluminescence by flow injection analysis (FIA)
192 following Obata et al. (1993). The FIA system was equipped with a Toyopearl AF Chelate 650M
193 resin. Sample concentrations were determined by standard addition and were verified by
194 analyzing 'Sampling and Analysis of Fe (SAFe)' reference seawater with each analytical run.
195 Our results for the reference seawater were in good agreement with the consensus values for
196 SAFe S: 0.090 ± 0.008 nmol L^{-1} (n=2) and SAFe D2: 1.043 ± 0.004 nmol L^{-1} (n=2). The
197 precision of the method varied between 4 - 8% (1 SD) and was determined by analyzing internal
198 reference seawater after every 10 samples. The blank of the FIA method was 0.028 ± 0.010 nmol
199 L^{-1} (n=12) and the limit of detection (LOD) determined by the product of the blank and three
200 times standard deviation of the blank was 0.058 nmol L^{-1}.
201
202 *Chlorophyll a*
203 Subsamples (300 or 400 mL) were collected from each of the triplicate bottles and
204 filtered through 25 mm diameter glass fiber filters (GF/F, Whatman). Filters were placed in 5 mL
205 of 90% acetone and extracted in the dark at 2°C for 24 hrs. Samples were equilibrated to room
206 temperature before measurement. Fluorescence at 685 nm was measured using a Turner Designs

TD-700 Field Fluorometer, calibrated with a Chl *a* standard (Sigma-Aldrich, C6144) dissolved in 90% acetone using the Welschmeyer (1994) filter setup.

^{14}C-based primary productivity

Primary productivity (PP) was determined using ^{14}C-labelled bicarbonate as a tracer for net inorganic carbon fixation (Steeman-Nielsen 1952). A subsample from each treatment bottle was collected into acid-cleaned, sample-rinsed 75 mL polycarbonate bottles and spiked with ^{14}C-bicarbonate to achieve a final activity of approximately 250 μCi L^{-1} (or 9.3 MBq L^{-1}, MP Biomedical #017441H). The bottles were incubated from dawn to dusk in the same on-deck incubator previously described. At the end of the daylight period, the entire sample volume was filtered through a 25 mm GF/F. The filters were placed into 20 mL borosilicate scintillation vials, acidified (1 mL, 2 mol L^{-1} hydrochloric acid) and vented for 24 hrs prior to the addition of scintillation cocktail (Ultima Gold LLT, Perkin-Elmer). Radioactivity was determined by liquid scintillation counting. Subsamples (250 µL) for total ^{14}C-radioactivity were collected from each incubation bottle and fixed in phenethylamine (Sigma-Aldrich #407267). Rates of carbon fixation are expressed as µmol C L^{-1} d^{-1}.

Active fluorescence

Fast Repetition Rate Fluorometry (FRRF) was utilized to evaluate possible changes in photophysiology in response to the availability of different N and Fe substrates, as described in Kolber et al. (1998). The FRRF instrument was operated with multiple excitation wavelengths (450 nm, 470 nm, 505 nm, and 530 nm) that allowed for the rapid assessment of photosystem II physiology in different groups of phytoplankton. Samples (500 mL) were first dark adapted (20

min) before conducting fluorescence measurements. Fluorescence transients were acquired in samples that were continuously recirculated through the instrument sample chamber. The sample chamber was exposed to FRRF excitation protocol composed of a series of microsecond-long flashlets of controlled excitation power. The saturation phase of the excitation was comprised of 100 flashlets at 2.5 microsecond intervals. With the pulse excitation power of 30,000 to 50,000 μmol quanta m^{-2} s^{-1}, the rate of excitation delivery to PSII centers far exceeded the capacity of photosynthetic electron transport between PSII and PSI. This resulted in a progressive saturation of the observed fluorescence transients within the first 40-60 flashlets, with a rate proportional to the functional absorption cross section at particular wavelength. The saturation phase was followed by 90 flashlets applied at exponentially-increasing time interval starting at 20 μs, over a period of 250 ms. As the average excitation power decreased, the fluorescence signal relaxed with a kinetics mostly defined by the rates of electron transport between PSII and PSI. Each sample measurement consisted of an average of 32 transients, and each sample was measured three times at each wavelength. Blanks were obtained by gently filtering sample water through a 0.2 μm syringe filter and processing it in the same manner as the samples. Recorded fluorescence transients were processed with FRRF software (http://soliense.com/) to estimate photosystem II maximum *in vivo* fluorescence (Fm), maximum photochemical efficiency (Fv/Fm), the functional absorption cross section (σ_{PSII}) for all Chl *a*-containing cells (excitation wavelength of 470 nm) and phycoerythrin-containing plankton (e.g. *Synechococcus*, excitation wavelength of 505 nm), and the kinetics of the PSII-PSI electron transport.

Flow cytometry

252 Samples (2 mL of seawater) for subsequent flow cytometric enumeration of picoplankton
253 were immediately fixed with glutaraldehyde (0.25% v/v final concentration) upon collection,
254 kept at room temperature in the dark for 15 min, then flash frozen and kept at -80°C until
255 processing. Abundances of *Prochlorococcus*, *Synechococcus*, photosynthetic picoeukaryotes
256 (PPEs), and heterotrophs were enumerated using a BD Biosciences Influx Cell Sorter (BD
257 Biosciences, San Jose, CA, USA) equipped with a 488 nm Sapphire laser (Coherent, Santa Clara,
258 CA, USA) using a 70 μm nozzle. All fixed seawater samples were pre-filtered using
259 a CellTrics® filter with 30 μm mesh (Partec, Swedesboro, NJ, USA). *Synechococcus*
260 populations were identified based on the presence of phycoerythrin (orange fluorescence; 572–
261 27 photomultiplier tube, PMT) and all other non-phycoerythrin populations were identified using
262 forward scatter (FSC) as a proxy for cell size and Chl *a* content (red fluorescence; 692–20 PMT).
263 To enumerate non-pigmented cells (heterotrophs), samples were stained with SYBR® Green I
264 nucleic acid stain (Lonza Inc., Allendale, NJ, USA) according to the protocol described in Marie
265 et al. 1999. To determine the abundances of non-pigmented heterotrophs with High Nucleic Acid
266 content (HNA cells), the abundance of *Prochlorococcus* and *Synechococcus* cells were
267 subtracted from all HNA cells. Data collection was triggered in the forward scatter (FSC)
268 channel for photosynthetic cells and in the green channel (531-40 PMT) for SYBR-stained cells.
269 Photosynthetic cells were counted for 10 min; SYBR-positive cells were counted for 1.5 min.
270 Cell counts were processed in FlowJo v10.0.7 (Tree Star, Inc., Ashland, OR, USA).
271
272 *DNA extraction*
273 1-2 L of seawater from each incubation bottle was filtered onto 0.2 μm Supor membrane
274 filters (Pall Corp., Ann Arbor, MI, USA) using peristaltic pumps. The filters were placed in

sterile 2.0 mL microcentrifuge tubes containing 0.5 and 1 mm diameter glass beads (Biospec, Bartlesville, OK, USA), flash frozen in liquid N_2, and stored at -80°C until DNA extraction. DNA was extracted using the Qiagen DNeasy Plant kit (Valencia, CA, USA), with modifications outlined in Moisander et al. (2008) to improve recovery of high quality DNA. The final wash steps and DNA elution were automated using a QIAcube robotic workstation (Qiagen). DNA quantity and quality was measured using a NanoDrop (Thermo Scientific, Waltham, MA, USA) with an average DNA yield 1100±900 ng L^{-1} seawater.

16S rRNA gene sequencing and sequence read processing

Community composition was analyzed based on sequences of the V3-V4 hypervariable region of the 16S rRNA gene using universal primers targeting Bacteria, Bakt_341F and Bakt_805R (Herlemann et al. 2011). Primers were modified with common sequence linkers (Moonsamy et al. 2013) to facilitate library preparation. PCR amplifications were carried out in triplicate 25 μL reactions for each sample, with the following reaction conditions: 1X Platinum Taq PCR buffer –Mg (Invitrogen, Carlsbad, CA), 2.5 mM $MgCl_2$, 200 μM dNTP mix, 0.25 μM of both forward and reverse primers, 3 U Platinum Taq DNA Polymerase (Invitrogen), and 1 uL of the DNA template. DNA was amplified using the following thermocycling conditions: initial denaturation at 95°C for 5 min, 25 cycles of denaturation at 95°C for 40 s, annealing at 53°C for 40 s, elongation at 72°C for 60 s, and a final elongation at 72°C for 7 min. Pooled amplicons underwent 10 more amplification cycles to add sequencing adaptors and sample-specific barcodes at the DNA Services Facility at the University of Illinois, Chicago, using the targeted amplicons sequencing approach described in Green et al. (2015). After the second round of PCR amplification performed by DNA Services at UIC, library concentrations were equalized using

SequalPrep purification plates (ThermoFisher Scientific). Paired-end reads were sequenced at the W.M. Keck Center for Comparative and Functional Genomics at the University of Illinois at Urbana-Champaign using Illumina MiSeq technology. Sequences of the 16S rRNA gene amplicons were obtained from a total of 91 samples that included samples in three replicates from T0, T24 and T48 for both experiments. There were on average 9986 reads per sample (median=9990, minimum=9664, and maximum=10340 reads per sample). De-multiplexed raw paired-end reads were merged using PEAR (Zhang et al. 2014). Assembled sequences were then quality filtered (split_libraries_fasta.py; phred score of 20) and chimeras were removed using a de novo approach (identify_chimeric_seqs.py) in QIIME (Caporaso et al. 2010). Operational taxonomic units (OTU) were defined at 99% nucleotide similarity using the usearch6.1 clustering method (Edgar 2010; pick_otus.py) and representative sequences were retrieved (pick_rep_set.py) in QIIME. The taxonomy of representative sequences was assigned using a Greengenes reference database (http://greengenes.secondgenome.com/downloads/database/13_5; DeSantis et al. 2006), and the assign_taxonomy.py QIIME script. We used the default parameters for the uclust consensus taxonomy assigner through QIIME (the minimum percent similarity for a taxonomic assignment was 0.9). The 16S rRNA gene sequences were deposited in Sequence Read Archive at National Center for Biotechnology Information (NCBI, http://www.ncbi.nlm.nih.gov/sra) under BioProject accession number PRJNA358607.

Oligotyping

The oligotyping approach separates individual taxa, 'oligotypes', within closely related organisms based on high entropy nucleotide positions in the 16S rRNA gene sequence (Eren et al. 2013). In order to define oligotypes for *Prochlorococcus* and *Synechococcus*, we used the

oligotyping pipeline version 2.0 (May 27, 2015) and followed the instructions available at http://oligotyping.org (Eren et al. 2013). The oligotyping analysis was performed separately for both *Prochlorococcus* and *Synechococcus*. A total of 395,666 and 10,271 reads were obtained for *Prochlorococcus* and *Synechococcus*, respectively, from samples taken at T0 and T48 in the two experiments. Before the oligotyping analysis, the sequences were aligned using PyNAST (Caporaso et al. 2010) and Greengenes 16S rRNA gene reference database (gg_13_5 version available at http://greengenes.secondgenome.com/). Shannon entropy calculations were followed by the oligotyping analysis, which was run until each oligotype had converged (as described in Eren et al. 2013). The following parameters were chosen for both *Prochlorococcus* and *Synechococcus* oligotyping analyses: a=0.1 and s=2, where 'a' is the minimum percent abundance of an oligotype in at least one sample and 's' is the minimum number of samples where an oligotype is expected to be present (Eren et al. 2013). The minimum substantial abundance criterion, M, determines the minimum abundance of the most abundant unique sequence in an oligotype and helps to reduce noise (Eren et al. 2013). For *Prochlorococcus* and *Synechococcus* oligotyping analyses, M was 100 and 20, respectively. To assign taxonomy, the representative sequences of the oligotypes were searched against the reference genome database at NCBI using blastn version 2.3.0+ (Altschul et al. 1990). The BLAST search was done with the default parameters, and all best hits were saved. Because some strains within the genera *Prochlorococcus* and *Synechococcus* have identical 16S rRNA V3-V4 region sequences, a representative sequence of an oligotype often was equally identical to several strains. We called a group of such identical strains an eStrain, and the strains within each eStrain are reported in Table S1. Note that the sequences belonging to one oligotype are identical at the selected nucleotide positions within the amplified ~441 nt region, but may vary at other positions within

the 16S rRNA gene. Next, the relative abundance of oligotypes was used to calculate the absolute abundance using the cell counts for *Prochlorococcus* and *Synechococcus,* and the absolute numbers were used in further analyses.

Shifts in community composition

The changes in composition of the heterotrophic microbial communities and *Prochlorococcus* and *Synechococcus* communities, were analyzed using the *Phyloseq* package (McMurdie and Holmes 2013) within R (The R Core Team 2013, http://www.r-project.org). For heterotrophic community analysis, phylum "Cyanobacteria" (that includes sequences from chloroplasts) were excluded, and the selected taxa were required to have a minimum of 50 reads total, resulting in 676090 sequences total in all samples (minimum of 6195, median of 7040, and maximum of 9493 sequences per sample). Ecological distances among the samples were estimated with the Bray-Curtis and Jaccard indices. To compare the community shifts, resulting from different treatments, Principal Coordinate Analysis (PCoA) was applied on the distance matrices. In addition, the relative read abundances for heterotrophic microbial communities were standardized to the median sequence depths (rarefied). There was little difference in the depth of sequencing among the samples (maximum difference <600 reads with a mean of ~10K reads per sample) and the PCoA results for standardized data were similar to the results from the non-standardized data.

Software

All statistical analyses were done in R (The R Core Team 2013, http://www.r-project.org): two-sample t-test for comparisons of means for Chl *a*, PP, abundances, and FRRF

367 measurements between treatments and controls and between treatments. To test for the observed
368 differences in community composition among treatments, analysis of similarities was done on
369 the Bray-Curtis dissimilarity distance matrix (*anosim* function within the "vegan" package in R,
370 Oksanen et al. 2016). The statistic R in analysis of similarities is based on the difference of mean
371 ranks between the groups and within groups, ranges from -1 to 1, and R value of 0 indicates
372 random groupings. In addition to analysis of similarities, analysis of variance (*adonis* function in
373 "vegan") was done on the Bray-Curtis dissimilarity matrix. Data were visualized using the
374 ggplot2 package (Wickham 2009) in R, and all final figures were prepared for publication using
375 Adobe Illustrator.
376
377 **Results**
378 *Initial conditions*
379 The physical and chemical conditions at the two experimental sites differed substantially. TZ
380 (Station 38) was located in the transition zone between the California Current and the NPSG
381 along the eastern margin of an anticyclonic eddy (Figs. 1a&b). GY (Station 52) was located in
382 the oligotrophic waters of the central gyre and further west in the NPSG in an area of relatively
383 low eddy activity (Fig. 1b). Both salinity and seawater temperature were higher at GY than at TZ
384 (Table 1). The mixed layer depth was twice as deep at GY (48 m) in comparison to TZ (24 m)
385 (Fig. 1c).
386 Concentrations of NO_3^-+NO_2^- in near-surface waters were low (<3 nmol L^{-1}) at both
387 experimental sites (Table 1) while concentrations of NH_4^+ were higher at TZ (58±3 nmol L^{-1} vs.
388 36±10 nmol L^{-1} at GY). Soluble reactive phosphorus (SRP) concentrations were approximately
389 three-fold higher and concentrations of $Si(OH)_4$ were 1.5-fold higher at TZ compared to GY.

390 Finally, surface concentrations of dissolved Fe were below detection (LOD=0.058 nmol L^{-1}) at
391 both sites.
392 The abundance of total picoplankton cells was approximately equal at the two
393 experimental stations (Table 1, 4.7±0.8 x 10^5 and 5.0±0.6 x 10^5 cells mL^{-1} at GY and TZ,
394 respectively) but the composition of the communities was somewhat different. Phytoplankton
395 cells were 1.5-fold more abundant at GY relative to TZ (Table 1) mainly due to
396 *Prochlorococcus*; however, the difference was not significant (1.6±0.5 x 10^5 cells mL^{-1} and
397 1.0±0.5 x 10^5 cells mL^{-1} at GY and TZ, respectively). *Synechococcus* was approximately 100-
398 times less abundant than *Prochlorococcus* at both sites (1.2±0.8 x 10^3 and 3.9±0.7 x 10^3 cells
399 mL^{-1} at GY and TZ, respectively). *Synechococcus* abundance was 3-times higher at TZ
400 compared to GY, accounting for 0.8% and 0.2% of total cells at each site, respectively.
401 Likewise, the abundance of photosynthetic picoeukaryotes (PPE) was low at both sites
402 (1.14±0.03 x 10^3 and 2.5±0.2 x 10^3 cells mL^{-1} at GY and TZ, respectively), with TZ having ~2.3-
403 times more PPE cells than GY. PPE accounted for ≤0.5% of the total cell population at either
404 site. Finally, heterotrophic bacteria were enumerated as either high nucleic acid (HNA)- or low
405 nucleic acid (LNA)-containing populations, the latter of which was more abundant (Table 1).
406 The abundances of each HNA and LNA cells were similar between the two sites (1.2±0.2 x 10^5
407 and 2.5±0.3 x 10^5 for HNA and LNA cells, respectively).
408 Despite the differences in physicochemical conditions and the composition of the microbial
409 communities, the initial concentrations of Chl *a* and rates of PP were similar at the two stations
410 (Table 1). In contrast, maximum photochemical efficiency of PSII measured at excitation
411 wavelength of 470 nm (Fv/Fm_{470}) was higher at TZ (0.51±0.01) than at GY (0.34±0.02), while

412 no significant difference was detected between stations with respect to functional absorption
413 cross-section of PSII ($\sigma_{PSII-470}$).
414
415 *Phytoplankton Chl* a *concentrations and PP rates*
416 All tested N forms and Fe alone resulted in significant increases in Chl *a* concentrations
417 and rates of PP after 48 hrs of incubation at both locations, and the response at GY was in
418 general larger than at TZ (Fig. 2). Additional nutrients (for example through the addition of Fe or
419 filtered deep water, FDW) did not enhance the response observed for the N forms further.
420 The largest increases in concentrations of Chl *a* at TZ after 48 hrs of incubation were
421 observed in response to urea and NH_4^+ additions (0.19±0.01 μg L^{-1}), >3.5-times higher in
422 comparison to the Control (no nutrient addition, Chl_{cnt}, 0.052±0.002 μg L^{-1}) (Fig. 2a). Addition
423 of NO_3^- produced a 1.4-times increase in Chl *a* over Chl_{cnt} at TZ. At GY, the urea addition
424 resulted in the largest responses in Chl *a* concentration (0.18±0.01 μg L^{-1}) compared to the Chl_{cnt}
425 (0.034±0.003 μg L^{-1}), followed by the NH_4^+ and NO_3^- additions (3-times higher relative to
426 Chl_{cnt})).
427 Changes in PP were similar to the Chl *a* responses in both experiments, with 4-times
428 higher carbon fixation rates observed in response to additions of urea and NH_4^+ at TZ (1.40±0.07
429 μmol C L^{-1} d^{-1}) and 8-times higher rates in response to urea at GY(1.3±0.1 μmol C L^{-1} d^{-1}) in
430 comparison to the Controls at 48 hours (PP_{cnt}; Fig. 2b). The NO_3^- addition at TZ resulted in 2.5-
431 times higher PP rates relative to the PP_{cnt}. Both NH_4^+ and NO_3^- yielded >5-times higher PP
432 relative to the PP_{cnt} after 48 hrs of incubation at GY.
433 In addition to stimulation by N substrates, the Fe addition alone produced a significant
434 increase in Chl *a* concentrations (40% increase over Chl_{cnt}) and rates of PP (>20% increase over

435 PP_{cnt}) at both locations after 48 hours of incubation (Fig. 2 and Table S2). However, the
436 additions of NO_3^- + Fe (N+Fe) and FDW stimulated Chl *a* concentrations and PP rates to the
437 same degree as the NO_3^- addition alone at both station (Fig. 2, Table S2).
438
439 *Photophysiology*
440 Use of FRRF to interrogate phytoplankton photophysiological responses (Fm, Fv/Fm and
441 σ_{PSII}) to nutrient amendments demonstrated that the phytoplankton community at both sites was
442 affected by the addition of the individual N compounds, and the response was stronger and more
443 variable at GY than at TZ (Fig. 3). Addition of Fe alone also had a stimulating effect on the
444 photosystem activity; however, N+Fe did not have an additional stimulating effect compared to
445 NO_3^- alone.
446 Fm at 470 nm (Fm_{470}; inclusive of all Chl-containing plankton) increased significantly
447 after 24 hrs of incubation in response to all N substrates in both experiments (Fig. 3). At TZ, all
448 N sources resulted in a similar increase in Fm_{470} relative to the Control by 48 hrs. At GY, urea,
449 NH_4^+ and N+Fe all resulted in large increases in Fm_{470} (300%) compared with the Control by 48
450 hrs, while the increase in the NO_3^- and FDW treatments was slightly less (200%). Finally, Fe
451 addition yielded a lower but significant (Table S3) increase in Fm_{470} (50% relative to the
452 Control) by 48 hrs at both locations.
453 The addition of the various N substrates also stimulated phycoerythrin-containing
454 phytoplankton (Fm_{505}), but the response to different N forms at the two locations varied (Fig 3).
455 Fm_{505} was significantly stimulated in the NO_3^- and NH_4^+ treatments by 24 hrs at both stations
456 while Fm_{505} increased in response to urea only at TZ. By 48 hrs at TZ, NH_4^+, NO_3^-, N+Fe and
457 FDW additions all increased the Fm_{505} response (>130%) relative to the Control (Fig. 3b). At

458 GY, additions of NH_4^+ and N+Fe resulted in a larger Fm_{505} response (>300% increase relative to
459 the Control; Fig. 3b), while the responses to urea, NO_3^- and FDW were slightly less (>200%
460 increase relative to the Control). Fe had a significant but weak effect on Fm_{505} by 48 hrs at both
461 stations (Fig. 3b, Table S3).

462 Fv/Fm was significantly influenced by all N forms and by Fe largely at GY. The initial
463 Fv/Fm_{470} was higher at the TZ station (0.51±0.01 and 0.34±0.02 at TZ and GY, respectively). At
464 GY, all N additions resulted in a significant increase in Fv/Fm_{470} in comparison to the Control by
465 24 hrs, with the highest (145%) increase in response to NO_3^- and NH_4^+ (Fig. 3c). At TZ, only the
466 NO_3^- addition resulted in a significant increase in Fv/Fm_{470} and only after 48 hrs (Fig. 3c and
467 Table S3). Similar to Fv/Fm_{470}, the initial Fv/Fm_{505} at GY (0.41±0.03) was lower than at TZ
468 (0.50±0.02). At GY, all N and Fe additions resulted in an increase in Fv/Fm_{505} similar to that of
469 Fv/Fm_{470} (Fig. 3d). However, in contrast to responses in Fv/Fm_{470}, Fv/Fm_{505} was weakly affected
470 by the three N forms by 24 hrs at TZ.

471 The response observed for σ_{PSII} to the additions of urea and NH_4^+ was anti-correlated
472 with the responses observed for Chl *a* concentrations and PP. σ_{PSII} observed at 470 nm
473 significantly decreased at TZ in response to the addition of both urea and NH_4^+ relative to the
474 Control (Fig. 3e); in contrast, σ_{PSII} decreased only in response to urea at the GY station.
475 Likewise, a significant decrease in response to urea was also observed for σ_{PSII} at 505 nm but
476 only at GY (Fig. 3f, Table S3). A weak stimulating effect (<30% of the Control) on σ_{PSII} was
477 observed for phytoplankton with 505 nm excitation wavelength in response to N+Fe and FDW
478 additions at GY and in response to N+Fe and NH_4^+ at TZ (Fig. 3e&f, Table S3).
479
480 *Response of the phytoplankton and bacterial groups*

Phytoplankton and non-photosynthetic bacteria had different qualitative and quantitative responses to N and Fe substrates, with variations depending on location.

All N forms resulted in increases in *Prochlorococcus* abundance at TZ and GY (Fig. 4a). The largest response at TZ was observed in the NH_4^+ and urea treatments ($2.2\pm0.3\ 10^5$ cells mL^{-1}), where *Prochlorococcus* abundance was 4-times higher than in the Control after 48 hrs. In the NO_3^-, N+Fe, and FDW treatments, *Prochlorococcus* abundance was 2-times higher than in the Control. At GY, urea produced the largest increase in *Prochlorococcus* abundance by 48 hrs ($2.8\pm0.1\ 10^5$ cells mL^{-1}, 3-times higher than the Control) followed by NO_3^- with 2-times higher *Prochlorococcus* abundance compared to the Control. The effects of NH_4^+, N+Fe, and FDW on *Prochlorococcus* abundances were less (~50% increase over the Control) at GY. Fe stimulated *Prochlorococcus* abundance at TZ (~40% increase over the Control) but not at GY.

Synechococcus abundance also increased significantly in response to the addition of urea, NO_3^-, N+Fe, and Fe at both stations, and the response to N was greatest at GY (Fig. 4b). *Synechococcus* abundances following the urea or NO_3^- additions were 3.5 ± 0.5 and $3.2\pm0.3\ 10^3$ cells mL^{-1} (>1.3-times higher than in the Controls) at TZ and GY, respectively. Addition of NH_4^+ resulted in a decrease in *Synechococcus* abundance at TZ and only a small increase at GY; however, the effect was not significantly different from the Control by 48 hrs at either station (Table S4). *Synechococcus* abundance at both locations responded to Fe additions. While not significantly different from the effect of N at TZ, the Fe effect was significantly lower than the effects of urea and NO_3^- at GY (Table S4). Notably, addition of N+Fe resulted in a significantly higher *Synechococcus* response in comparison to Fe alone at both stations (Fig. 4b, Table S4).

PPE abundance increased significantly in response to all N forms and to Fe at both stations. Overall larger increases in PPE abundance were observed at GY (Fig. 4c) than at TZ.

504 NO_3^- resulted in a high degree of variability between the replicates at TZ, which contributed to a
505 lower statistical significance ($t_{(2)}$=2.4, p=0.06). PPE abundances in response to all N at TZ were
506 ~1.5-times higher than in the Control and were similar for all nutrients including Fe (average
507 PPE abundance in all N and Fe additions was ~2.1±0.4 10^3 cells mL^{-1}). At GY by 48 hours,
508 additions of NH_4^+, urea, NO_3^-, N+Fe, and FDW resulted in >100% increases in PPE abundance
509 relative to the Control and Fe-alone treatment (average ~1.1±0.2 10^3 cells mL^{-1} in the N
510 additions; Fig. 4c).
511 HNA abundance responded to additions of NH_4^+, NO_3^-, and N+Fe at both stations (up to
512 125% increase over the Control by 48 hrs, Fig. 4d). At GY, the HNA cells also increased 1.5-
513 times the Control in response to the FDW addition. The increase in HNA abundance at GY, but
514 not at TZ, was significant by 24 hrs (Table S4). In contrast to the HNA cells, only the N+Fe
515 addition at TZ station resulted in a significant increase (38% relative to the Control) in the
516 abundance of LNA cells by 48 hrs (Fig. 4e). No significant increase in the LNA cell abundance
517 was observed at GY (Fig. 4e, Table S4).
518
519 *Shift in microbial community composition*
520 To further evaluate the effect of N on the microbial communities at these two sites, and to
521 assess whether differences in microbial community composition accompanied the observed
522 changes in PP, Chl *a*, FRRF, and cell abundance, we amplified and sequenced the V3-V4
523 hypervariable region of the 16S rRNA gene. Based on the 16S rRNA gene relative abundances,
524 the initial microbial community composition (Control T0) at the genus level was similar at both
525 locations and was dominated by Cyanobacteria (genus *Prochlorococcus*, 31-34% of total 16S
526 rRNA gene sequences) and *Alphaproteobacteria* (family *Pelagibacteraceae*, 30-33% of total

16S rRNA gene sequences), followed by other *Alphaproteobacteria* (no taxonomic assignment, 7-8% of total 16S rRNA gene sequences), *Gammaproteobacteria* (*Halomonadaceae*: *C*. Portiera, 5-7% of total 16S rRNA gene sequences), and *Actinobacteria* (*Acidimicrobiales*: OCS155, 2-3% of total 16S rRNA gene sequences) (Fig. 5a). *Synechococcus* was a minor component of the microbial community at both locations (0.7% of total 16S rRNA sequences). Relative abundances of chloroplast 16S rRNA sequences varied between the two locations. At TZ, abundances of *Haptophyceae* and *Stramenopiles* each were 1.9% of total 16S rRNA gene sequences. At GY, relative abundances of *Haptophyceae* and *Stramenopiles* in the initial community were 1.1% and 0.8%, respectively.

A shift in microbial community composition at the genus level in response to all N additions was detected within 48 hrs in both experiments with the strongest response to NH_4^+ (Fig. 5). Both Jaccard and Bray-Curtis ecological indices produced similar results (Fig. 5b and S1a). Differences in the Bray-Curtis dissimilarities between treatments were significant (difference of mean ranks between the groups $R>0.77$, $p<0.001$ in both experiments). At both locations, the response to all N forms was characterized by the increase in relative abundance of representatives from the Gammaproteobacteria families *Alteromonadaceae* and *Oceanospirillaceae* (Fig. 5a). At TZ, the relative abundance of *Alteromonadaceae* (unassigned genus) increased from 0.2% in the Control to 41%, 55% and 57% of all reads in the urea, NH_4^+, and NO_3^- additions at T48, respectively. At GY, the relative abundance of *Alteromonadaceae* (unassigned genus) increased from 0.3% in the Control to 15%, 34% and 36% of all reads in the urea, NO_3^-, and NH_4^+ additions at T48, respectively. Relative abundance of *Oleispira* (family *Oceanospirillaceae*) increased significantly in the N additions, but only at GY: from 0.1% in the Control to 9%, 10% and 20% of all reads in NH_4^+, urea, and NO_3^- additions at T48, respectively.

550 The relative abundance of another *Oceanospirillaceae* genus (*Oleibacter*) increased from
551 undetectable in the Control to as much as 5% of all reads in the N additions at TZ. Addition of
552 NH_4^+ resulted in the most distinct microbial community, with the shift observed within 24 hrs at
553 both stations (Fig. 5a&b). Relative abundance of 16S rRNA gene sequences from representatives
554 of the genus *Phaeobacter* (Alphaproteobacteria: *Rhodobacteraceae*) were associated with the
555 NH_4^+ additions and increased from undetectable in the Control to 5% and 19% of all reads in the
556 NH_4^+ addition in both GY and TZ at T48, respectively (Fig. S1c). Addition of urea resulted in a
557 less pronounced change in microbial community composition, especially at TZ. Finally, Fe
558 addition did not significantly influence community composition at both locations.
559 The shift in microbial community composition in response to all N forms at GY was
560 faster than at TZ and detected by 24 hrs after the addition of nutrients (Figs. 5a&b). Samples
561 taken 24 hrs after the start of the incubation experiment at TZ were most similar to the Controls
562 and T0 samples. In contrast, T48 samples from treatments with any N addition at TZ clustered
563 separately from the T0 and T24 samples, Controls, and Fe addition treatment. At GY, all of the
564 N addition treatments clustered separately from the Controls, T0, and Fe addition within 24 hrs.
565
566 *Response of picocyanobacteria to N*
567 Given the great genetic diversity within marine microbial genera (e.g. Kashtan et al.
568 2014), we examined changes in abundance of individual taxa within *Prochlorococcus* and
569 *Synechococcus* populations at high resolution by using an oligotyping approach (Eren et al.
570 2013). The responses to different N forms and Fe varied between and within *Prochlorococcus*
571 and *Synechococcus* genera.

572 *Prochlorococcus* populations differed between the two locations (Fig. 6a). A total of 31
573 oligotypes were identified in *Prochlorococcus* communities across both experiments based on 7
574 nucleotide positions with high entropy (as described in the Methods). The *Prochlorococcus*
575 communities at TZ and GY were dominated by strains from the High Light I (HLI) and High
576 Light II (HLII) clades, respectively. The oligotypes MED4-oligo1 (100% identical to
577 *Prochlorococcus* MED4, HLI) and MIT9515-oligo1 (100% identical to *Prochlorococcus*
578 MIT9515, HLI) were on average 74% and 10%, respectively, of all of the *Prochlorococcus*
579 sequences in the Control T0 sample at TZ (Table 2). At GY, these oligotypes comprised 1% of
580 total *Prochlorococcus* sequences in the Control T0 (Table 2). The most abundant oligotype at
581 GY, MIT9301-oligo1 (100% identical to *Prochlorococcus* MIT9301, HLII, and strains with
582 similar sequence of the 16S rRNA gene region, Table S1), comprised on average 66% of the
583 *Prochlorococcus* sequences. The next most abundant, the MIT9312-oligo1 oligotype (100%
584 identical to *Prochlorococcus* MIT9312, HLII, and related strains, Table S1), was on average
585 22% of the *Prochlorococcus* sequences at GY station. Both of the most abundant oligotypes at
586 GY were <1% of the sequences in the Control T0 from TZ (Table 2). Representatives of the Low
587 Light I (LLI) clade were present at both locations, although only as minor portions of the
588 community (Table 2).
589 The addition of different N forms had differential effects on the *Prochlorococcus*
590 populations in both experiments by 48 hrs (Figs. 6b-d). While urea addition resulted in a
591 consistent increase in abundance of all *Prochlorococcus* oligotypes and clades, NH_4^+ and NO_3^-
592 resulted in variable responses within the *Prochlorococcus* communities and between the two
593 locations. Differences in the Bray-Curtis dissimilarities for *Prochlorococcus* communities
594 between treatments were higher than within treatments (analysis of similarities for TZ: R=0.36,

595 p=0.007, and GY: R=0.51, p=0.002, see Methods). The Bray-Curtis dissimilarity index showed
596 that urea and NH_4^+ additions resulted in a shift in the *Prochlorococcus* community composition
597 that was most distinct from the effects of the rest of the treatments and Controls at TZ, while the
598 urea and NO_3^- additions resulted in the strongest shift in comparison to the effects of the rest of
599 the treatments (and Controls) at GY (Fig. 6b). These patterns paralleled the general response of
600 total *Prochlorococcus* abundance (measured by flow cytometry) and were observed for the most
601 abundant *Prochlorococcus* oligotypes in each experiment (Fig. 6c&d). However, the minor
602 oligotype NATL1A-oligo1 (LLI) had a larger response to urea and NO_3^- than to NH_4^+ at TZ (Fig.
603 6d). At GY, some members of HLII, HLI and LLI clades had no significant responses to NH_4^+
604 (Fig. 6c and S2).

605 Some *Prochlorococcus* oligotypes had different responses to nutrient amendments
606 between the two sites. For example, the two dominant oligotypes at TZ, MED4-oligo1 and
607 MIT9515-oligo1, had the greatest response to urea and NH_4^+ (Fig. 6d). However, although they
608 were minor (<1%) components of the *Prochlorococcus* community at GY, these oligotypes had
609 the greatest responses to urea and NO_3^- (Fig. 6c and S2). The responses by *Prochlorococcus*
610 PAC1-oligo1 (LLI) also varied between the two sites (Fig. 6d and S2).

611 Similar to *Prochlorococcus, Synechococcus* communities at the two locations were
612 distinct; however, the most dominant *Synechococcus* oligotypes were the same at the two
613 locations (Fig. 7a). A total of 11 oligotypes were distinguished for *Synechococcus* based on 11
614 nucleotide positions with high entropy. *Synechococcus* oligotypes derived from both clades II
615 and IV were most abundant at TZ, whereas *Synechococcus* oligotypes from clade II were most
616 abundant at GY. *Synechococcus* oligotype CC9605-oligo1, with 100% identity to *Synechococcus*
617 CC9605 (clade II), was the most abundant at both locations, constituting on average of 35% and

618 61% of *Synechococcus* 16S rRNA gene sequences at TZ and GY, respectively (Table 2).
619 Another oligotype from clade II, CC9605-oligo2, was also present at both stations (Table 2).
620 Two oligotypes derived from clade IV (CC9902-oligo1 and CC9902-oligo2 with 100% and
621 99.7% identity, respectively, to *Synechococcus* CC9902) contributed 39% to the *Synechococcus*
622 community at TZ. The least abundant oligotypes present at both stations included representatives
623 from clade V (Table 2).
624 N additions had a larger effect on *Synechococcus* community composition at GY than at
625 TZ (Fig. 7b). Differences in the Bray-Curtis dissimilarities for *Synechococcus* communities
626 between treatments were significantly higher than within treatments at GY (analysis of
627 similarities for GY: R=0.54, p=0.001 compared to TZ: R=0.19, p=0.07). The Bray-Curtis
628 dissimilarity index showed a weak separation of samples with NO_3^-, urea, N+Fe, and FDW
629 additions from the Controls and samples with NH_4^+ and Fe additions at TZ. At GY, all nutrients,
630 including Fe, resulted in a strong shift in the *Synechococcus* community, with the urea addition
631 resulting in the most distinct responses compared to other nutrient additions.
632 Similar to *Prochlorococcus*, N forms had a differential effect on *Synechococcus*
633 oligotypes, resulting in distinct *Synechococcus* populations by 48 hr (Figs. 7c&d). The response
634 of oligotypes also varied between the sites. Consistent with the response in total *Synechococcus*
635 abundance, the dominant oligotype CC9902-oligo1 (clade IV) responded to NO_3^-, urea, Fe, and
636 FDW at TZ. In contrast, the oligotype CC9605-oligo5 (clade II) had a weak increase in
637 abundance in response to urea availability relative to the Control at TZ (Fig. 7d). However, all N
638 forms and Fe affected this oligotype abundance at GY (Fig. 7c), with the largest effect seen in
639 the NO_3^- and N+Fe additions. Urea had the largest effect on the less abundant oligotype CC9605-
640 oligo2 (clade II) at GY. Moreover, less abundant oligotypes had distinct responses compared to

641 the responses of the dominant oligotypes. For example, oligotype KORDI100-oligo1 (Clade V)
642 had a significant increase in cell abundance only in response to N+Fe at TZ (Fig. 7d).
643
644 **Discussion**
645 The effect of N availability on biological processes in the ocean is one of the most
646 studied topics in marine microbiology; however, we still know little about the complex
647 interactions between the diverse microbial communities and different N compounds used by
648 specific microorganisms. We investigated the effects of NO_3^-, NH_4^+, and urea as sources of N on
649 microbial community activity (PP and photosynthetic efficiency), and community composition
650 (based on major microbial group cell counts and 16S rRNA gene sequence) in the open ocean
651 waters of the North Pacific Ocean. All N forms tested had significant effects on microbial
652 communities at the investigated sites in the NPSG within 48 hrs (Table 3). Limitation of PP and
653 maximum photochemical efficiency of PSII by N has been reported in other low-latitude
654 oligotrophic waters, such as in the North Atlantic Ocean (Graziano et al. 1996; Moore et al.
655 2006, 2008; Davey et al. 2008). Moreover, N was the major limiting nutrient constraining total
656 phytoplankton biomass in the Western South Pacific Ocean (Moisander et al. 2012) and in the
657 South Pacific Gyre (Van Wambeke et al. 2008). In addition to N, either P or Fe can co-limit
658 picoplankton cell growth in the North Atlantic (Davey et al. 2008). While the effect of SRP was
659 not specifically tested in our study, the addition of FDW (which had elevated SRP and NO_3^-
660 concentrations, Table 1) resulted in similar responses as the addition of N alone, suggesting that
661 P did not co-limit plankton biomass or productivity during our experiments.
662
663 *Stimulating effect of urea on phytoplankton*

664 The importance of urea as an N source for phytoplankton was demonstrated decades ago
665 (McCarthy et al. 1972b; Price and Harrison 1988; Antia et al. 1991; Fan et al. 2003). The urease
666 gene has been found in a variety of marine microorganisms, including the cyanobacteria
667 *Synechococcus* and *Prochlorococcus*, eukaryotic phytoplankton (haptophytes, diatoms,
668 prasinophytes), and heterotrophic bacteria (*Roseobacteraceae*, *Pelagibacter*,
669 Gammaproteobacteria HTCC2207) (Baker et al. 2009; Collier et al. 2009; Solomon et al. 2010).
670 Urea concentrations in the surface open oceans appear highly variable in space and time, ranging
671 from 0.3 to 0.7 μmol N L^{-1} (Bronk et al. 2002; Painter et al. 2008). In the current study, urea was
672 added at much higher concentrations (2.5 and 5.0 μmol of N L^{-1}) than previously reported in situ
673 concentrations; however, our results demonstrated that all major groups of phytoplankton
674 responded to the urea additions, with responses differing between the two locations examined
675 (Table 3). Previous studies have also described variable responses in rates of uptake and growth
676 in phytoplankton when urea was supplied as the sole N source (Cochlan and Harrison 1991;
677 Lomas and Glibert 2000; Moore et al. 2002; Fan et al. 2003; Solomon et al. 2010).
678 Our results suggest that urea may be an important N source for *Prochlorococcus* (Figs.
679 6&7), which is responsible for a large fraction of PP in the open oceans (Vaulot et al. 1995;
680 Campbell et al. 1997; DuRand et al. 2001). *Prochlorococcus* clades HLI and HLII dominated at
681 the TZ and GY stations, respectively, consistent with the observations that these clades occupy
682 different niches, with the shift from the HLI to the HLII clade reported at the threshold of ~23°C
683 in summer (Farrant et al. 2016; Larkin et al. 2016). *Prochlorococcus* HLI and HLII are the most
684 abundant *Prochlorococcus* clades (Johnson et al. 2006) and the majority of sequenced
685 *Prochlorococcus* genomes have urea utilization and transporter genes (Kettler et al. 2007;
686 Scanlan et al. 2009). The results of our study showed that both clades responded significantly to

687 urea additions, demonstrating large increases in abundances, >300% relative to the Controls.
688 The oligotyping analysis of *Prochlorococcus* 16S rRNA gene sequences further showed that
689 *Prochlorococcus* community composition was strongly influenced by urea additions at both
690 sites. The high transcription of the urea transporter gene in natural populations of
691 *Prochlorococcus* found in metatranscriptomic studies (Frias-Lopez et al. 2008; Gifford et al.
692 2011; Shi et al. 2011) suggests that *Prochlorococcus* actively acquire urea. Indeed, rates of urea
693 uptake by *Prochlorococcus* in the Sargasso Sea were found to be similar or faster than NH_4^+
694 uptake rates (Casey et al. 2007), and a significant relationship was observed between
695 *Prochloroccocus* abundances and bulk urea uptake rates in the Northern Atlantic Ocean (Painter
696 et al. 2008). While utilization of urea by picocyanobacteria has been shown before (Rippka et al.
697 2000; Moore et al. 2002), our study suggests that urea may be an important source of N
698 supporting the growth of natural populations of *Prochlorococcus*.
699
700 *Variable responses of phytoplankton to NH_4^+ and NO_3^-*
701 In contrast to urea, the effects of NO_3^- and NH_4^+ on phytoplankton communities varied
702 between the sites. The addition of NH_4^+ significantly stimulated rates of PP both at the TZ and
703 GY stations. At GY, both NO_3^- and NH_4^+ additions resulted in the similar degree of enhancement
704 in PP, but responses to these additions had a less stimulating effect than that of urea. The PP
705 response pattern at TZ was paralleled by changes in *Prochlorococcus* cell abundance and
706 community composition. The different responses to the two N forms were likely the result of
707 uptake preferences by different phytoplankton groups for NO_3^- and NH_4^+, as well as different
708 degrees of Fe limitation experienced among the phytoplankton groups at TZ (discussed below).

709 Genetic and physiological differences may help explain the differential responses of
710 *Prochlorococcus* populations to NH_4^+ and NO_3^- between the two experimental sites. Genes
711 encoding pathways for NO_3^-/NO_2^- assimilation have been found in some *Prochlorococcus* HL
712 and LL strains, and these strains are able to grow solely on NO_3^- as an N source (Martiny et al.
713 2009; Berube et al. 2015). Thus, not surprisingly, naturally-occurring *Prochlorococcus*
714 populations from HLI, HLII, and LLI clades responded to NO_3^- additions at low NH_4^+
715 concentrations at both stations in our study. Laboratory studies indicate that *Prochlorococcus*
716 growth on NO_3^- is slower than growth on NH_4^+ (Berube et al. 2015) and such results could
717 explain the differences in cell abundances in response to NO_3^- and NH_4^+ additions at TZ.
718 Additionally, the genome of *Prochlorococcus* MIT9515 (HLI), a strain that was abundant at TZ,
719 has two copies of the *amt* gene which encodes an NH_4^+ transporter (Scanlan et al. 2009) and this
720 strain may be more competitive for NH_4^+ than the strains that were present at GY station. In
721 contrast, the genome of *Prochlorococcus* MIT0604 (HLII, with the V3-V4 region of the 16S
722 rRNA gene sequence 100% identical to *Prochlorococcus* MIT9301, the eStrain that was
723 dominant at GY) has two clusters of NO_3^- assimilation genes (Berube et al. 2015). Finally,
724 another HLII strain (SB strain) present at GY has the most extensive gene suite for N utilization,
725 including NO_3^-, urea, and cyanate assimilation genes (Berube et al. 2015). In addition to the
726 genetic and physiological differences, microbial interactions likely influenced the observed
727 changes in abundance. For example, it is possible that NO_3^- additions may have stimulated
728 growth of mixotrophic eukaryotes that consumed *Prochlorococcus* cells (Hartmann et al. 2013).
729 In general, the N-limitation of *Prochlorococcus* cell abundance observed in the present study
730 contrasted with results observed in the Western South Pacific Ocean where *Prochlorococcus*

731 HLII responded to Fe and P (Moisander et al. 2012), a finding that may reflect lower N:Fe or
732 N:P supply ratios in the northern hemisphere (Ward et al. 2013).
733 It was surprising that *Synechococcus* abundance showed little response to the NH_4^+
734 addition. NH_4^+ is thought to be the preferred N substrate by cyanobacteria over NO_3^- because of
735 the higher energetic cost for reduction and assimilation of NO_3^-. However, culture studies
736 showed that under sub-saturating irradiance, growth rates of marine *Synechococcus* on NO_3^-
737 were similar to growth rates on NH_4^+ (Collier et al. 2012). Considering that *Prochlorococcus* and
738 heterotrophic bacteria were orders of magnitude more abundant than *Synechococcus* at both
739 stations, and that *Synechococcus* cells have a lower surface area to volume ratio than
740 *Prochlorococcus* (Morel et al. 1993), *Synechococcus* may have been at a competitive
741 disadvantage for NH_4^+ uptake. However, the fact that ~50% of the added NH_4^+ remained after 48
742 hrs of incubation (Table S5) suggests that *Synechococcus* preferred NO_3^- as an N source,
743 although the mechanism for N substrate preference remains unclear (Collier et al. 2012).
744 In contrast to *Synechococcus*, the photosynthetic picoeukaryotes showed the greatest
745 increase in abundance in the NH_4^+ addition, but only at GY. The lack of a PPE response to NH_4^+
746 at TZ may be related to Fe availability (see below). A preference for NH_4^+ over NO_3^- and urea
747 has been previously shown for PPEs in culture, such as the prasinophyte *Micromonas* (Cochlan
748 and Harrison 1991). Interestingly, the prasinophytes *Micromonas* and *Ostreococcus* have genes
749 for two types of the NH_4^+ transporters (AMT), one of which is similar to bacterial *amt* (Derelle et
750 al. 2006; McDonald et al. 2010). Transcription of this AMT gene is up-regulated in response to
751 N-depletion (McDonald et al. 2010). Likewise, transcription of the NH_4^+ transporter genes in
752 response to N-depletion has also been shown for diatoms (Allen et al. 2005; Bowler et al. 2008).
753 The data presented here supports the observations of previous studies that eukaryotic

754 phytoplankton can successfully compete for NH_4^+ with smaller bacterial cells (Bradley et al.
755 2010).
756
757 *Fe limitation of phytoplankton growth and activity in the CCS*
758 Fe availability affected the abundance of all groups of phytoplankton and rates of PP at
759 TZ. Fe limitation of phytoplankton growth in the CCS is believed to be due to the rapid depletion
760 of Fe relative to NO_3^- in the upwelled waters that travel offshore as filaments (Bruland et al.
761 2001; Biller and Bruland 2013). In addition, the TZ site was in an anticyclonic eddy containing
762 open ocean water with relatively high SRP, but otherwise low nutrient and Chl *a* concentrations.
763 The mixing of open ocean water at the sampling site is further supported by the mixture of
764 coastal and open ocean phytoplankton communities found at this site. For example, the coastal
765 *Synechococcus* clade IV, usually prevalent in colder nutrient-rich waters, was present at the same
766 abundance as *Synechococcus* clade II, which is the dominant open ocean clade (Sohm et al.
767 2016). The high abundance of *Prochlorococcus* at this site also indicated an input of oligotrophic
768 gyre waters. Thus, the mixing of the oligotrophic gyre waters at TZ may have contributed to the
769 low Fe availability.
770 The genetic differences between the communities at the two stations is likely an
771 additional factor contributing to the stronger response to Fe at TZ. For example, coastal strains of
772 phytoplankton are adapted to have higher cellular Fe quotas than open ocean strains (Brand
773 1991; Sunda et al. 1991; Strzepek and Harrison 2004). Moreover, *Prochlorococcus* MED4
774 (HLI), which was abundant at TZ, has been shown to be especially sensitive to Fe availability
775 (Thompson et al. 2011). Finally, *Prochlorococcus* has a larger number of genes for coping with
776 low Fe environments than *Synechococcus* (Rocap et al. 2003; Scanlan et al. 2009), which may

777 explain why *Prochlorococcus* had a greater response to N than to Fe additions, in contrast to
778 *Synechococcus* at TZ. Thus, a combination of factors, genetic and environmental, may have
779 resulted in the strong community response to Fe at TZ. These results provide further support for
780 Fe limitation of phytoplankton growth in the CCS transition zone.

781 Furthermore, some microbial populations were most likely N and Fe co-limited at TZ. An
782 independent type of co-limitation of biomass (Arrigo 2005; Saito et al. 2008) may explain why
783 the addition of N and Fe together did not enhance the response in Chl *a* and primary productivity
784 relative to N or Fe additions alone. If only a small fraction of the community are N and Fe co-
785 limited in comparison to the N-limited fraction, then the effect of N+Fe may not be significant in
786 bulk measurements. The responses by the *Synechococcus* oligotypes support this hypothesis: The
787 oligotype identical to *Synechococcus* KORDI-100 (clade V) had greater relative abundances in
788 N+Fe in comparison to the Fe or N additions alone. However, this oligotype comprised only 5%
789 of the total *Synechococcus* population, and thus did not contribute significantly to the responses
790 in total *Synechococcus* biomass. The two other *Synechococcus* oligotypes at TZ (originating
791 from clades II and IV) showed similar responses to N+Fe, Fe, or NO_3^-. These were the most
792 abundant *Synechococcus* oligotypes at TZ and likely comprised many sub-populations that could
793 not be distinguished at the 16S rRNA gene resolution. Thus, using the high resolution
794 oligotyping approach allowed us to distinguish the diversity of responses within microbial
795 populations, such as to nutrient co-limitation, which were not reflected in the bulk
796 measurements.

797

798 *Responses of heterotrophic microbial communities to N substrates*

799 The heterotrophic community responded to N forms differently than the phototrophic
800 community. The NH_4^+ followed by the NO_3^- additions at both locations resulted in the strongest
801 shifts in heterotrophic community composition, as estimated from 16S rRNA gene relative
802 abundances (Table 3). Additionally, HNA cell abundances increased in the NO_3^- and NH_4^+
803 additions at both sites regardless of the phytoplankton response (Table 3). The shift was largely
804 due to the increase in the relative abundance of Gammaproteobacteria (*Oceanospirillaceae,*
805 *Alteromonadaceae,* and *Vibrionaceae*) and Alphaproteobacteria (*Phaeobacter*), the copiotrophic
806 microbial taxa known to respond rapidly to enrichments of surface seawater with nutrients or
807 associated with phytoplankton blooms (González et al. 2000; Shi et al. 2012; Beier et al. 2014;
808 El-Swais et al. 2015; Sosa et al. 2015). Smaller in size than some phytoplankton cells in general,
809 heterotrophic bacteria may have a competitive advantage by taking up available NH_4^+ and NO_3^-
810 rapidly, thereby actively competing for macronutrients, as has been reported in many other
811 studies (Eppley et al. 1977; Wheeler and Kirchman 1986; Kirchman 1994; Mills et al. 2008;
812 Bradley et al. 2010).
813
814 *Differences between the TZ and GY stations*
815 The greatest differences in microbial community responses to N additions between the
816 two locations were in the timing and degree of the responses. The shift in heterotrophic microbial
817 community composition at GY was observed earlier than at TZ. This may be due to the distinct
818 phototrophic communities at each location. For example, *Prochlorococcus* HLI and
819 *Synechococcus* Clades II and IV were dominant at TZ, and *Prochlorococcus* HLII and
820 *Synechococcus* Clade II were dominant at GY. However, our study suggests that the microbial
821 community was under more severe nutrient limitation at GY than at TZ. The nutricline at GY

822 was deeper than at TZ, and the microbes at GY had likely been nutrient limited longer than those
823 at the TZ station. The low initial Fv/Fm of the phototrophic community at GY and the significant
824 and rapid (in 24 hrs) increase in Fv/Fm upon N additions suggest that new N contributed to the
825 building of new photosynthetic proteins and that photosynthetic activity at GY was strongly N-
826 limited (Suggett et al. 2009). The increase in PP following N additions was also significantly
827 greater at GY than at TZ. As previously shown in cultures, N pre-conditioning affects how fast
828 phytoplankton respond to N (Conway et al. 1976; Price and Harrison 1988). Additionally,
829 phytoplankton species have the ability to change substrate affinities and uptake potentials
830 depending on the degree of nutrient limitation (Conway and Harrison 1977). Thus, microbial
831 community composition and N pre-conditioning may determine the timing and degree of the
832 responses to N substrates in the North Pacific.
833
834 **Conclusions**
835 N substrates have differential effects on different phytoplankton groups, and the degree
836 and rapidity of the responses depend on the pre-existing physicochemical conditions (e.g. Price
837 and Harrison 1988). Our study extends previous findings by using a combination of techniques
838 to measure total microbial community physiological and functional responses as well as shifts in
839 microbial community composition and changes in abundance of phytoplankton populations at
840 high taxonomic resolution. The results of our study indicate that N availability limited PP and
841 accumulation of microbial biomass during our sampling in the open ocean waters of the North
842 Pacific. Moreover, we observed distinct differences in rates of PP, accumulation of biomass, and
843 community composition in response to additions of urea, NH_4^+, and NO_3^-. The growth of some
844 populations of phytoplankton, especially *Synechococcus* and PPE, was also limited by Fe in the

CCS region. Our results also suggest the heterotrophic microbial community successfully competed for inorganic N sources at both experimental sites. Finally, besides the differences in community composition, the pre-existing conditions at each site likely influenced the timing and degree of the responses to N perturbations by both phytoplankton and heterotrophic community.

There is strong evidence that future oceans will experience changes in temperature and N supply (Kim et al. 2014). The genetics of populations determines how environmental factors affect their ecologies and evolution (e.g. Larkin et al. 2016), and the results of our study imply that changes in N substrate availability favors different components of the phytoplankton community in different oceanic regions. More importantly, because phytoplankton taxa vary in elemental stoichiometry (Sterner and Elser 2002; Bertilsson et al 2003; Heldal et al. 2003), physiology (e.g. Moore et al. 2002), viral resistance (Stoddart et al. 2007) and DOM production (Becker et al. 2014), changes in phytoplankton community composition would impact biogeochemical cycles, as well as ecological processes. The results of our study underline the importance to better understand the complex interactions between diverse microbial populations and nutrient availability in the oceans.

Acknowledgements

We thank the captain, crew and technicians of the R/V *New Horizon* for assistance and support during the research cruise. We thank Mary Hogan (UCSC) for helping in preparations for the cruises and DNA extraction, Joaquin Pampin Baro (GEOMAR) for providing support for the trace-metal free work, Dr. Stefan Green and his staff at the DNA Services Facility (the University of Illinois, Chicago) for next generation sequencing consultation, Ed Boring (UCSC) for bioinformatics assistance. In addition, Susan Curless, Brenner Wai, Alexa Nelson, and Stu

868 Goldberg all provided laboratory support of this project. This work was supported by awards
869 from the National Science Foundation Dimensions in Biodiversity program (1241221), Center
870 for Microbial Oceanography: Research and Education (NSF EF0424599), and the Deutsche
871 Forschungsgemeinschaft as part of Sonderforschungsbereich 754: 'Climate-Biogeochemistry
872 Interactions in the Tropical Ocean' (to EPA).
873

874 **References**

875 Allen, A. E. 2005. Beyond sequence homology: Redundant ammonium transporters in a marine
876 diatom are not functionally equivalent. *J. Phycol*. **41**: 4-6.
877 Allen, A. E., M. G. Booth, M. E. Frischer, P. G. Verity, J. P. Zehr, and S. Zani. 2001. Diversity
878 and detection of nitrate assimilation genes in marine bacteria. *Appl. Environ. Microbiol*.
879 **67**: 5343-5348.
880 Allen, A. E., A. Vardi, and C. Bowler. 2006. An ecological and evolutionary context for
881 integrated nitrogen metabolism and related signaling pathways in marine diatoms. *Curr.*
882 *Opin. Plant Biol.* **9**: 264-273.
883 Altschul, S. F., W. Gish, W. Miller, E. W. Myers, and D. J. Lipman. 1990. Basic local alignment
884 search tool. *J. Mol. Biol*. **215**: 403-410.
885 Aluwihare, L. I., and T. Meador. 2008. Chemical composition of marine dissolved organic
886 nitrogen, p. 95-140. In D. G. Capone, D. A. Bronk, M. R. Mulholland and E. J. Carpenter
887 [eds.], *Nitrogen in the Marine Environment*, 2nd ed. Elsevier Academic Press Inc.
888 Antia, N. J., P. J. Harrison, and L. Oliveira. 1991. The role of dissolved organic nitrogen in
889 phytoplankton nutrition, cell biology and ecology. *Phycologia* **30**: 1-89.
890 Arrigo, K. R. 2005. Marine microorganisms and global nutrient cycles. *Nature* **437**: 349-355.
891 Baker, K. M., C. J. Gobler, and J. L. Collier. 2009. Urease gene sequences from algae and
892 heterotrophic bacteria in axenic and nonaxenic phytoplankton cultures. *J. Phycol*. **45**:
893 625-634.
894 Becker, J. W., and others. 2014. Closely related phytoplankton species produce similar suites of
895 dissolved organic matter. *Front. Microbiol*. **5**: 14.
896 Beier, S., A. R. Rivers, and M. A. Moran, I. Obernosterer. 2015. The transcriptional response of
897 prokaryotes to phytoplankton-derived dissolved organic matter in seawater. *Environ.*
898 *Microbiol.* **17**: 3466–3480.
899 Bertilsson, S., O. Berglund, D. M. Karl, and S. W. Chisholm. 2003. Elemental composition of
900 marine *Prochlorococcus* and *Synechococcus*: Implications for the ecological
901 stoichiometry of the sea. *Limnol. Oceanogr*. **48**: 1721-1731.
902 Berube, P. M., and others. 2015. Physiology and evolution of nitrate acquisition in
903 *Prochlorococcus*. *ISME J*. **9**: 1195-1207.
904 Bidigare, R. R. 1983. Nitrogen excretion by marine zooplankton, p. 385-409. In E. J. Carpenter
905 and D. G. Capone [eds.], *Nitrogen in the marine environment*. Academic Press.
906 Biller, D. V., and K. W. Bruland. 2013. Sources and distributions of Mn, Fe, Co, Ni, Cu, Zn, and
907 Cd relative to macronutrients along the central California coast during the spring and
908 summer upwelling season. *Mar. Chem*. **155:** 50-70.
909 Biller, D. V., and K. W. Bruland. 2014. The central California Current transition zone: A broad
910 region exhibiting evidence for iron limitation. *Prog. Oceanogr.* **120**: 370-382.
911 Bonnet, S., and others. 2008. Nutrient limitation of primary productivity in the Southeast Pacific
912 (BIOSOPE cruise). *Biogeosciences* **5**: 215-225.
913 Böttjer, D., J.E. Dore, D.M. Karl, R.M. Letelier, C. Mahaffey, S.T. Wilson, and M.J. Church.
914 2016. Temporal variability in nitrogen fixation and particulate nitrogen export at Station
915 ALOHA. *Limnol. Oceanogr*. doi: 10.1002/lno.10386.
916 Bowler, C., and others. 2008. The *Phaeodactylum* genome reveals the evolutionary history of
917 diatom genomes. *Nature* **456**: 239-244.

Bradley, P. B., and others. 2010. Inorganic and organic nitrogen uptake by phytoplankton and heterotrophic bacteria in the stratified Mid-Atlantic Bight. *Estuarine Coastal Shelf Sci.* **88**: 429-441.

Brand, L. E. 1991. Minimum iron requirements of marine-phytoplankton and the implications for the biogeochemical control of new production. *Limnol. Oceanogr*. **36**: 1756-1771.

Bronk, D. A. 2002. Dynamics of DON, p 153–247. In: D. A. Hansell and C. A. Carlson [eds.], *Biogeochemistry of marine dissolved organic matter*. Academic Press.

Bronk, D. A., P. M. Glibert, T. C. Malone, S. Banahan, and E. Sahlsten. 1998. Inorganic and organic nitrogen cycling in Chesapeake Bay: autotrophic versus heterotrophic processes and relationships to carbon flux. *Aquat. Microb. Ecol*. **15:** 177-189.

Bruland, K. W., E. L. Rue, and G. J. Smith. 2001. Iron and macronutrients in California coastal upwelling regimes: Implications for diatom blooms. *Limnol. Oceanogr*. **46**: 1661-1674.

Campbell, L., H. B. Liu, H. A. Nolla, and D. Vaulot. 1997. Annual variability of phytoplankton and bacteria in the subtropical North Pacific Ocean at Station ALOHA during the 1991-1994 ENSO event. *Deep-Sea Res.*, *Part I*. **44**: 167-192.

Caporaso, J. G., and others. 2010. QIIME allows analysis of high-throughput community sequencing data. *Nat. Methods*. **7**: 335-336.

Capotondi, A., M. A. Alexander, N. A. Bond, E. N. Curchitser, and J. D. Scott. 2012. Enhanced upper ocean stratification with climate change in the CMIP3 models. *J. Geophys. Res.*: *Oceans* **117**: C04031.

Casey, J. R., M. W. Lomas, J. Mandecki, and D. E. Walker. 2007. *Prochlorococcus* contributes to new production in the Sargasso Sea deep chlorophyll maximum. *Geophys. Res. Lett.* **34**: L10604.

Chisholm, S. W., R. J. Olson, E. R. Zettler, R. Goericke, J. B. Waterbury, and N. A. Welschmeyer. 1988. A novel free-living prochlorophyte abundant in the oceanic euphotic zone. *Nature* **334**: 340-343.

Cochlan, W. P., and P. J. Harrison. 1991. Uptake of nitrate, ammonium, and urea by nitrogen-starved cultures of *Micromonas-pusilla* (*Prasinophyceae*) - transient responses. *J. Phycol*. **27**: 673-679.

Collier, J. L., K. M. Baker, and S. L. Bell. 2009. Diversity of urea-degrading microorganisms in open-ocean and estuarine planktonic communities. *Environ. Microbiol*. **11**: 3118-3131.

Collier, J. L., R. Lovindeer, Y. Xi, J. C. Radway, and R. A. Armstrong. 2012. Differences in growth and physiology of marine *Synechococcus* (Cyanobacteria) on nitrate versus ammonium are not determined solely by nitrogen source redox state. *J. Phycol.* **48**: 106-116.

Conway, H. L., and P. J. Harrison. 1977. Marine diatoms grown in chemostats under silicate or ammonium limitation. 4. Transient-response of *Chaetoceros-debilis, Skeletonema-costatum,* and *Thalassiosira-gravida* to a single addition of limiting nutrient. *Mar. Biol*. **43**: 33-43.

Conway, H. L., P. J. Harrison, and C. O. Davis. 1976. Marine diatoms grown in chemostats under silicate or ammonium limitation. 2. Transient-response of *Skeletonema-costatum* to a single addition of limiting nutrient. *Mar. Biol*. **35**: 187-199.

Corner, E. D. S., and B. S. Newell. 1967. On nutrition and metabolism of zooplankton. 4. Forms of nitrogen excreted by *Calanus*. *J. Mar. Biol. Assoc. U. K.* **47**: 113-120.

Davey, M., G. A. Tarran, M. M. Mills, C. Ridame, R. J. Geider, and J. LaRoche. 2008. Nutrient limitation of picophytoplankton photosynthesis and growth in the tropical North Atlantic.

964 *Limnol. Oceanogr*. **53:** 1722-1733.
965 Derelle, E., and others. 2006. Genome analysis of the smallest free-living eukaryote
966 *Ostreococcus tauri* unveils many unique features. *Proc. Natl. Acad. Sci. U. S. A.* **103**:
967 11647-11652.
968 DeSantis, T. Z., and others. 2006. Greengenes, a chimera-checked 16S rRNA gene database and
969 workbench compatible with ARB. *Appl. Environ. Microbiol*. **72**: 5069-5072.
970 Dore, J. E., T. Houlihan, D. V. Hebel, G. Tien, L. Tupas, and D. M. Karl. 1996. Freezing as a
971 method of sample preservation for the analysis of dissolved inorganic nutrients in
972 seawater. *Mar. Chem*. **53**: 173-185.
973 Dore, J. E., and D. M. Karl. 1996. Nitrification in the euphotic zone as a source for nitrite,
974 nitrate, and nitrous oxide at Station ALOHA. *Limnol. Oceanogr*. **41**: 1619-1628.
975 Duce, R. A., and others. 2008. Impacts of atmospheric anthropogenic nitrogen on the open
976 ocean. *Science* **320**: 893-897.
977 Dugdale, R. C., and J. J. Goering. 1967. Uptake of new and regenerated forms of nitrogen in
978 primary productivity. *Limnol. Oceanogr*. **12**: 196-206.
979 DuRand, M. D., R. J. Olson, and S. W. Chisholm. 2001. Phytoplankton population dynamics at
980 the Bermuda Atlantic Time-series station in the Sargasso Sea. *Deep-Sea Res., Part II.* **48**:
981 1983-2003.
982 Edgar, R. C. 2010. Search and clustering orders of magnitude faster than BLAST. *Bioinformatics*
983 **26**: 2460-2461.
984 El-Swais, H., K. A. Dunn, J. P. Bielawski, W. K. W. Li, and D. A. Walsh. 2015. Seasonal
985 assemblages and short-lived blooms incoastal north-west Atlantic Ocean
986 bacterioplankton. *Environ. Microbiol*. **17**: 3642–3661.
987 Eppley, R. W., and B. J. Peterson. 1979. Particulate organic-matter flux and planktonic new
988 production in the deep ocean. *Nature* **282**: 677-680.
989 Eppley, R. W., J. H. Sharp, E. H. Renger, M. J. Perry, and W. G. Harrison. 1977. Nitrogen
990 assimilation by phytoplankton and other microorganisms in surface waters of central
991 North Pacific Ocean. *Mar. Biol.* **39**: 111-120.
992 Eren, A. M., and others. 2013. Oligotyping: differentiating between closely related microbial
993 taxa using 16S rRNA gene data. *Meth. Ecol. Evol*. **4**: 1111-1119.
994 Fan, C., P. M. Glibert, J. Alexander, and M. W. Lomas. 2003. Characterization of urease activity
995 in three marine phytoplankton species, *Aureococcus anophagefferens, Prorocentrum*
996 *minimum,* and *Thalassiosira weissflogii*. *Mar. Biol.* **142**: 949-958.
997 Farrant, G. K., and others. 2016. Delineating ecologically significant taxonomic units from
998 global patterns of marine picocyanobacteria. *Proc. Natl. Acad. Sci. U. S. A.* **113**: E3365-
999 E3374.
1000 Fawcett, S. E., M. Lomas, J. R. Casey, B. B. Ward, and D. M. Sigman. 2011. Assimilation of
1001 upwelled nitrate by small eukaryotes in the Sargasso Sea. *Nat. Geosci*. **4**: 717-722.
1002 Frias-Lopez, J., and others. 2008. Microbial community gene expression in ocean surface waters.
1003 *Proc. Natl. Acad. Sci. U. S. A.* **105**: 3805-3810.
1004 Garside, C. 1982. A chemi-luminescent technique for the determination of nanomolar
1005 concentrations of nitrate and nitrite in sea-water. *Mar. Chem*. **11**: 159-167.
1006 Gifford, S. M., S. Sharma, J. M. Rinta-Kanto, and M. A. Moran. 2011. Quantitative analysis of a
1007 deeply sequenced marine microbial metatranscriptome. *ISME J.* **5**: 461-472.
1008 González, J. M., R. Simó, R.Massana, J. S. Covert, E. O. Casamayor, C. Pedrós-Alió, and M. A.
1009 Moran. 2000. Bacterial community structure associated with a

dimethylsulfoniopropionate-producing North Atlantic algal bloom. *Appl. Environ. Microbiol.* **66**: 4237-4246.

Graziano, L. M., R. J. Geider, W. K. W. Li, and M. Olaizola. 1996. Nitrogen limitation of North Atlantic phytoplankton: Analysis of physiological condition in nutrient enrichment experiments. *Aquat. Microb. Ecol*. **11**: 53-64.

Green, S. J., R. Venkatramanan, and A. Naqib. 2015. Deconstructing the Polymerase Chain Reaction: understanding and correcting bias associated with primer degeneracies and primer-template mismatches. *PLoS One* **10**: 21.

Gruber, N., and J. N. Galloway. 2008. An Earth-system perspective of the global nitrogen cycle. *Nature* **451**: 293-296.

Hallam, S. J., and others. 2006. Pathways of carbon assimilation and ammonia oxidation suggested by environmental genomic analyses of marine *Crenarchaeota*. *PLoS Biol.* **4**: 520-536.

Hansell, D. A., and J. J. Goering. 1989. A method for estimating uptake and production-rates for urea in seawater using [^{14}C] urea and [^{15}N] urea. *Can. J. Fish. Aquat. Sci.* **46**: 198-202.

Hartmann, M., M. V. Zubkov, D. J. Scanlan, and C. Lepere. 2013. In situ interactions between photosynthetic picoeukaryotes and bacterioplankton in the Atlantic Ocean: evidence for mixotrophy. *Environ. Microbiol. Rep.* **5**: 835-840.

Heldal, M., D. J. Scanlan, S. Norland, F. Thingstad, and N. H. Mann. 2003. Elemental composition of single cells of various strains of marine *Prochlorococcus* and *Synechococcus* using X-ray microanalysis. *Limnol. Oceanogr*. **48**: 1732-1743.

Herlemann, D. P. R., M. Labrenz, K. Jurgens, S. Bertilsson, J. J. Waniek, and A. F. Andersson. 2011. Transitions in bacterial communities along the 2000 km salinity gradient of the Baltic Sea. *ISME J.* **5**: 1571-1579.

Johnson, Z. I., E. R. Zinser, A. Coe, N. P. McNulty, E. M. S. Woodward, and S. W. Chisholm. 2006. Niche partitioning among *Prochlorococcus* ecotypes along ocean-scale environmental gradients. *Science* **311**: 1737-1740.

Karner, M. B., E. F. DeLong, and D. M. Karl. 2001. Archaeal dominance in the mesopelagic zone of the Pacific Ocean. *Nature* **409**: 507-510.

Kettler, G. C., and others. 2007. Patterns and implications of gene gain and loss in the evolution of *Prochlorococcus*. *PLoS Genet.* **3**: 2515-2528.

Kim, I. N., and others. 2014. Increasing anthropogenic nitrogen in the North Pacific Ocean. *Science* **346**: 1102-1106.

Kirchman, D. L. 1994. The uptake of inorganic nutrients by heterotrophic bacteria. *Microbiol. Ecol.* **28**: 255-271.

Kolber, Z. S., O. Prasil, and P. G. Falkowski. 1998. Measurements of variable chlorophyll fluorescence using fast repetition rate techniques: defining methodology and experimental protocols. *Biochim*. *Biophys. Acta, Bioenerg*. **1367**: 88-106.

Larkin, A. A., and others. 2016. Niche partitioning and biogeography of high light adapted *Prochlorococcus* across taxonomic ranks in the North Pacific. *ISME J*. **10**: 1555-1567.

Li, Q. P., J. Z. Zhang, F. J. Millero, and D. A. Hansell. 2005. Continuous colorimetric determination of trace ammonium in seawater with a long-path liquid waveguide capillary cell. *Mar. Chem*. **96**: 73-85.

Lomas, M. W., and P. M. Glibert. 2000. Comparisons of nitrate uptake, storage, and reduction in marine diatoms and flagellates. *J. Phycol.* **36**: 903-913.

Marie, D., F Partensky, D. Vaulot, and C. Brussaard. 1999. Enumeration of phytoplankton,

bacteria, and viruses in marine samples, p. 11.11.1-11.11.15. In J. P. Robinson [ed], *Current protocols in cytometry*. John Wiley and Sons, Inc.
Martiny, A. C., S. Kathuria, and P. M. Berube. 2009. Widespread metabolic potential for nitrite and nitrate assimilation among *Prochlorococcus* ecotypes. *Proc. Natl. Acad. Sci. U. S. A.* **106**: 10787-10792.
Mayzaud, P. 1973. Respiration and nitrogen excretion of zooplankton. 2. Studies of metabolic characteristics of starved animals. *Mar. Biol.* **21**: 19-28.
McCarthy, J. J. 1972a. Uptake of urea by marine phytoplankton. *J. Phycol*. **8**: 216-222.
---. 1972b. Uptake of urea by natural populations of marine phytoplankton. *Limnol. Oceanogr.* **17**: 738-748.
McCarthy, J. J., and R. W. Eppley. 1972. Comparison of chemical, isotopic, and enzymatic methods for measuring nitrogen assimilation of marine phytoplankton. *Limnol. Oceanogr.* **17**: 371-382.
McDonald, S. M., J. N. Plant, and A. Z. Worden. 2010. The mixed lineage nature of nitrogen transport and assimilation in marine eukaryotic phytoplankton: a case study of *Micromonas*. *Mol. Biol. Evol*. **27**: 2268-2283.
McMurdie, P. J., and S. Holmes. 2013. phyloseq: An R package for reproducible interactive analysis and graphics of microbiome census data. *PLoS One* **8**: 11.
Mills, M. M., and others. 2008. Nitrogen and phosphorus co-limitation of bacterial productivity and growth in the oligotrophic subtropical North Atlantic. *Limnol. Oceanogr*. **53:** 824-834.
Mills, M. M., C. Ridame, M. Davey, J. La Roche, and R. J. Geider. 2004. Iron and phosphorus co-limit nitrogen fixation in the eastern tropical North Atlantic. *Nature* **429**: 292-294.
Mitamura, O., and Y. Saijo. 1981. Studies on the seasonal-changes of dissolved organic-carbon, nitrogen, phosphorus and urea concentrations in lake Biwa. *Arch. Hydrobiol*. **91**: 1-14.
Moisander, P. H., R. A. Beinart, M. Voss, and J. P. Zehr. 2008. Diversity and abundance of diazotrophic microorganisms in the South China Sea during intermonsoon. *ISME J.* **2**: 954-967.
Moisander, P. H., R. F. Zhang, E. A. Boyle, I. Hewson, J. P. Montoya, and J. P. Zehr. 2012. Analogous nutrient limitations in unicellular diazotrophs and *Prochlorococcus* in the South Pacific Ocean. *ISME J*. **6:** 733-744.
Montoya, J. P., E. J. Carpenter, and D. G. Capone. 2002. Nitrogen fixation and nitrogen isotope abundances in zooplankton of the oligotrophic North Atlantic. *Limnol. Oceanogr*. **47**: 1617-1628.
Moonsamy, P. V., and others. 2013. High throughput HLA genotyping using 454 sequencing and the Fluidigm Access Array (TM) system for simplified amplicon library preparation. *Tissue Antigens* **81**: 141-149.
Moore, C. M., and others. 2013. Processes and patterns of oceanic nutrient limitation. *Nat. Geosci*. **6**: 701-710.
Moore, C. M., and others. 2008. Relative influence of nitrogen and phosphorus availability on phytoplankton physiology and productivity in the oligotrophic sub-tropical North Atlantic Ocean. *Limnol. Oceanogr*. **53**: 291-305.
Moore, L. R., A. F. Post, G. Rocap, and S. W. Chisholm. 2002. Utilization of different nitrogen sources by the marine cyanobacteria *Prochlorococcus* and *Synechococcus*. *Limnol. Oceanogr.* **47**: 989-996.
Morel, A., Y. H. Ahn, F. Partensky, D. Vaulot, and H. Claustre. 1993. *Prochlorococcus* and

Synechococcus - a comparative-study of their optical-properties in relation to their size and pigmentation. *J. Mar. Res*. **51**: 617-649.
Morris, R. M., and others. 2002. SAR11 clade dominates ocean surface bacterioplankton communities. *Nature* **420**: 806-810.
Mulholland, M. R., and M. W. Lomas. 2008. Nitrogen uptake and assimilation, p. 303-384. In D. G. Capone, D. A. Bronk, M. R. Mulholland and E. J. Carpenter [eds.], *Nitrogen in the Marine Environment*, 2nd Edition. Elsevier Academic Press Inc.
Obata, H., H. Karatani, and E. Nakayama. 1993. Automated-determination of iron in seawater by chelating resin concentration and chemiluminescence detection. *Anal. Chem*. **65**: 1524-1528.
Oksanen, J., and others. 2016. vegan: Community Ecology Package. R package version 2.4-1. https://CRAN.R-project.org/package=vegan.
Ortega-Retuerta, E., W. H. Jeffrey, J. F. Ghiglione, and F. Joux. 2012. Evidence of heterotrophic prokaryotic activity limitation by nitrogen in the Western Arctic Ocean during summer. *Polar Biol*. **35**: 785-794.
Price, N. M., and P. J. Harrison. 1988. Urea uptake by Sargasso Sea phytoplankton - saturated and in situ uptake rates. *Deep-Sea Res., Part II.* **35**: 1579-1593.
Quay, P. D., C. Peacock, K. Björkman, and D. M. Karl. 2010. Measuring primary production rates in the ocean: Enigmatic results between incubation and non-incubation methods at Station ALOHA. *Glob. Biogeochem. Cycles* **24**: GB3014. doi:10.1029/2009GB003665.
Rippka, R., and others. 2000. *Prochlorococcus marinus* Chisholm et al. 1992 subsp pastoris subsp nov strain PCC 9511, the first axenic chlorophyll a(2)/b(2)-containing cyanobacterium (Oxyphotobacteria). *Int. J. Syst. Evol. Microbiol*. **50**: 1833-1847.
Rocap, G., and others. 2003. Genome divergence in two *Prochlorococcus* ecotypes reflects oceanic niche differentiation. *Nature* **424**: 1042-1047.
Sahlsten, E. 1987. Nitrogenous nutrition in the euphotic zone of the central North Pacific Gyre. *Mar. Biol.* **96**: 433-439.
Saito, M. A., T. J. Goepfert, and J. T. Ritt. 2008. Some thoughts on the concept of colimitation: Three definitions and the importance of bioavailability. *Limnol. Oceanogr.* **53**: 276-290.
Scanlan, D. J., and others. 2009. Ecological genomics of marine picocyanobacteria. Microbiol. *Mol. Biol. Rev*. **73**: 249-299.
Shi, Y. M., J. McCarren, and E. F. DeLong. 2012. Transcriptional responses of surface water marinemicrobial assemblages to deep-sea water amendment. *Environ. Microbiol*. **14**: 191–206.
Shi, Y. M., G. W. Tyson, J. M. Eppley, and E. F. DeLong. 2011. Integrated metatranscriptomic and metagenomic analyses of stratified microbial assemblages in the open ocean. *ISME J*. **5**: 999-1013.
Sohm, J. A., and others. 2016. Co-occurring *Synechococcus* ecotypes occupy four major oceanic regimes defined by temperature, macronutrients and iron. *ISME J.* **10**: 333-345.
Solomon, C. M., J. L. Collier, G. M. Berg, and P. M. Glibert. 2010. Role of urea in microbial metabolism in aquatic systems: a biochemical and molecular review. *Aquat. Microb. Ecol.* **59**: 67-88.
Sosa, O. A., S. M. Gifford, D. J. Repeta, and E. F. DeLong. 2015. High molecular weight dissolved organic matter enrichment selects for methylotrophs in dilution to extinction cultures. *ISME J*. **9**: 2725–2739.
Steeman-Nielsen, E. 1952. The use of radioactive carbon (C14) for measuring organic

production in the sea. *J. Cons. Int. Explor. Mer*. **18**: 117-140.
Sterner, R.W. and J.J. Elser. 2002. *Ecological Stoichiometry: The Biology of Elements from Molecules to Biosphere.* Princeton University Press. Princeton, N.J.
Stoddard, L. I., J. B. H. Martiny, and M. F. Marston. 2007. Selection and characterization of cyanophage resistance in marine *Synechococcus* strains. *Appl. Environ. Microbiol*. **73**: 5516-5522.
Strickland, J. D. H. and T. R. Parsons. 1972. *A practical handbook of seawater analysis*. Second Edition, Bulletin 167. Fisheries Research Board of Canada, Ottawa.
Strzepek, R. F., and P. J. Harrison. 2004. Photosynthetic architecture differs in coastal and oceanic diatoms. *Nature* **431**: 689-692.
Suggett, D. J., C. M. Moore, A. E. Hickman, and R. J. Geider. 2009. Interpretation of fast repetition rate (FRR) fluorescence: signatures of phytoplankton community structure versus physiological state. *Mar. Ecol.: Prog. Ser.* **376**: 1-19.
Sunda, W. G., D. G. Swift, and S. A. Huntsman. 1991. Low iron requirement for growth in oceanic phytoplankton. *Nature* **351**: 55-57.
Thompson, A. W., K. Huang, M. A. Saito, and S. W. Chisholm. 2011. Transcriptome response of high- and low-light-adapted *Prochlorococcus* strains to changing iron availability. *ISME J*. **5**: 1580-1594.
Vaulot, D., D. Marie, R. J. Olson, and S. W. Chisholm. 1995. Growth of *Prochlorococcus*, a photosynthetic prokaryote, in the equatorial pacific-ocean. *Science* **268**: 1480-1482.
Van Wambeke, F., S. Bonnet, T. Moutin, P. Raimbault, G. Alarcon, and C. Guieu. 2008. Factors limiting heterotrophic bacterial production in the southern Pacific Ocean. *Biogeosciences* **5**: 833-845.
Ward, B. A., S. Dutkiewicz, C. M. Moore, and M. J. Follows. 2013. Iron, phosphorus, and nitrogen supply ratios define the biogeography of nitrogen fixation. *Limnol. Oceanogr*. **58**: 2059-2075.
Waterbury, J. B., S. W. Watson, R. R. L. Guillard, and L. E. Brand. 1979. Widespread occurrence of a unicellular, marine, planktonic cyanobacterium. *Nature* **277**: 293-294.
Welschmeyer, N. A. 1994. Fluorometric analysis of chlorophyll-*a* in the presence of chlorophyll-*b* and pheopigments. *Limnol. Oceanogr*. **39**: 1985-1992.
Wheeler, P. A., and D. L. Kirchman. 1986. Utilization of inorganic and organic nitrogen by bacteria in marine systems. *Limnol. Oceanogr.* **31**: 998-1009.
Wickham, H. 2009. *ggplot2: Elegant graphics for data analysis*. Springer-Verlag New York.
Worden, A. Z., J. K. Nolan, and B. Palenik. 2004. Assessing the dynamics and ecology of marine picophytoplankton: The importance of the eukaryotic component. *Limnol. Oceanogr*. **49**: 168-179.
Yool, A., A. P. Martin, C. Fernandez, and D. R. Clark. 2007. The significance of nitrification for oceanic new production. *Nature* **447**: 999-1002.
Zehr, J. P., and R. M.Kudela. 2011. Nitrogen cycle of the open ocean: from genes to ecosystems. *Annu. Rev. Mar. Sci.* **3**:197-225.
Zhang, J. J., K. Kobert, T. Flouri, and A. Stamatakis. 2014. PEAR: a fast and accurate Illumina Paired-End reAd mergeR. *Bioinformatics* **30**: 614-620.
Zhu, Y., D. X. Yuan, Y. M. Huang, J. Ma, S. C. Feng, and K. N. Lin. 2014. A modified method for on-line determination of trace ammonium in seawater with a long-path liquid waveguide capillary cell and spectrophotometric detection. *Mar. Chem.* **162**: 114-121.

Figure legends

Figure 1. Geographic locations in the North Pacific (a), sea surface height anomaly (b) and potential density profiles (c) of the two stations where nutrient addition experiments were conducted in August of 2014. Station 38 was in the western part of transition zone of California Current System (station TZ), and Station 52 was in the oligotrophic North Pacific Subtropical Gyre (station GY).

Figure 2. Phytoplankton community responses to N compounds and Fe at two stations in the NPSG. (a) Chlorophyll *a*, (b) rates of ^{14}C-PP measured after 48 hrs of incubation at the GY and TZ stations. The significantly different means (t-test, n=3, $p<0.05$) are indicated with unique small letters where letter 'a' indicates values not-significantly different from the control. FDW: 0.2 μm filtered 600 m water. The dashed lines show measurements at T0 in the control (no amendments). The dotted and dotdash lines in (b) show measurements at T0 in the N + Fe and FDW additions, respectively.

Figure 3. Phytoplankton photosystem II physiology responses to N compounds and Fe in the NPSG. (a and b) Maximum *in vivo* fluorescence yield (Fm); (c and d) maximum photochemical efficiency of PSII (Fv/Fm); (e and f) functional absorption cross-section of PSII (σ_{PII}) measured at 470 nm (a, c, e) and 505 nm (b, d, f) excitation wavelength in response to nutrient additions at the GY and TZ stations. The dashed lines show measurements at T0 in the control (no amendments). The significantly different means (t-test, n=3, $p<0.05$) are indicated with unique small letters where letter 'a' indicates values not-significantly different from the control. FDW: 0.2 μm filtered 600 m water.

Figure 4. Intergroup and spatial variability among phytoplankton and bacteria in responses to N compounds and Fe additions. Cell counts for (a) *Synechococcus*, (b) *Prochlorococcus,* (c) photosynthetic picoeukaryotes (PPE), (d) high nucleic acid containing bacteria (HNA) and (e) low nucleic acid containing bacteria (LNA) for all treatments measured 48 h after nutrient additions at the GY and TZ stations. The significantly different means (t-test, $n=3$, $p<0.05$) are indicated with unique small letters where letter 'a' indicates values not-significantly different from the control. FDW: 0.2 μm filtered 600 m water.

Figure 5. Nitrogen additions resulted in a shift in microbial composition by 48 hrs in the NPSG. (a) Microbial community composition based on the relative abundance of the 16S rRNA gene copy at the genus level in the experiments at the GY and TZ stations. Only top 30 abundant genera are listed. Each sample represents a mean of 16S rRNA gene copy relative abundance from three replicates. *ua* indicates unassigned taxa. (b) PCoA on Bray-Curtis distance measures among the samples for heterotrophic microbial community composition at the GY and TZ stations.

Figure 6. Differential responses of *Prochlorococcus* oligotypes to N compounds. (a) Distinct *Prochlorococcus* communities were present at the GY (left panel) and TZ stations (right panel). Abundances of *Prochlorococcus* oligotypes, cells mL^{-1} (Y axis), were estimated based on 16S rRNA gene amplicon sequencing, oligotyping analysis and cell counts. Oligotypes were assigned to Clade (X axis) and eStrain (legend) based on the highest nucleotide identity, where each eStrain represents a group of *Prochlorococcus* strains with 100% nucleotide identity in the V3-V4 region of the 16S rRNA gene sequence. (b) PCoA analysis on Bray-Curtis distance indices

1240 for *Prochlorococcus* community composition at T48 as a function of nutrient addition at the GY
1241 and TZ stations. (c and d) Responses in abundance of the selected *Prochlorococcus* oligotypes to
1242 nutrients at T48 at GY (c) and TZ (d). The dashed line shows abundances of each oligotype at
1243 T0.
1244
1245 **Figure 7.** Differential responses of *Synechococcus* oligotypes to N compounds. (a) Distinct
1246 *Synechococcus* communities were present at the GY (left panel) and TZ stations (right panel).
1247 Abundances of *Synechococcus* oligotypes, cells mL^{-1} (Y axis), were estimated based on 16S
1248 rRNA gene amplicon sequencing, oligotyping analysis and cell counts. Oligotypes were assigned
1249 to Clade (X axis) and eStrain (legend) based on the highest nucleotide identity, where each
1250 eStrain represents a group of *Synechococcus* strains with 100% nucleotide identity in the V3-V4
1251 region of the 16S rRNA gene sequence. (b) PCoA analysis on Bray-Curtis distance indices for
1252 *Synechococcus* community composition at T48 as a function of nutrient addition at the GY and
1253 TZ stations. (c and d) Responses in abundance of the selected *Synechococcus* oligotypes to
1254 nutrients at T48 at the GY (c) and TZ stations (d). The dashed line shows abundances of each
1255 oligotype at T0.

Tables

Table 1. Initial conditions at the two hydrographic stations where N amendment experiments were conducted.

		GY station	TZ station
Date		8/29/14	8/24/14
Location	Latitude (ddm)	27.281	33.502
	Longitude (ddm)	-140.382	-129.37
Physics	Temperature, °C	23.84±0.01	19.50±0.04
	Salinity	35.41±0.01	33.47±0.01
Nutrients	NO_3^-+NO_2^-, nmol L^{-1}	2.4±0.7	2.5±0.4
	NH_4^+, nmol L^{-1} *	36±10	58±3
	SRP, µmol L^{-1} ***	0.094±0.005	0.272±0.005
	$Si(OH)_4$, µmol L^{-1} ***	1.35±0.02	2.14±0.01
	Fe, nmol L^{-1}	below LOD[b]	below LOD[b]
Phytoplankton activity	Chl *a,* µg L^{-1}	0.058±0.001	0.057±0.003
	^{14}C-PP, µmol C L^{-1} d^{-1}	0.33±0.02	0.34±0.01
	Fm_{470}	3.4±0.2	3.6±0.3
	Fv/Fm_{470} **	0.34±0.02	0.51±0.01
	$\sigma_{PSII-470}$ x10^{-20} m^{-2} $quanta^{-1}$	850±40	900±40
Cell abundances	Phytoplankton total, mL^{-1}	1.6±0.5 x 10^5	1.1±0.5 x 10^5
	Prochlorococcus, mL^{-1}	1.6±0.5 x 10^5 (30.8%)	1.0±0.5 x 10^5 (20.3%)
	Synechococcus, mL^{-1} *	1.2±0.8 x 10^3 (0.2%)	3.9±0.7 x 10^3 (0.8%)
	Photosynthetic picoeukaryotes, mL^{-1} *	1.14±0.03 x 10^3 (0.2%)	2.5±0.2 x 10^3 (0.5%)
	HNA cells, mL^{-1}	1.2±0.1 x 10^5 (23.1%)	1.3±0.2 x 10^5 (25.3%)
	LNA cells, mL^{-1}	2.4±0.2 x 10^5 (46.2%)	2.6±0.3 x 10^5 (53.1%)
	Total cells[a], mL^{-1}	5.2±0.5 x 10^5	5.0±0.6 x 10^5

Concentrations of nutrients are shown as an average (±standard deviation) of three replicates. Chl *a* – chlorophyll *a* concentration; ^{14}C-PP – primary productivity rates; HNA – high nucleic acid cells; LNA – low nucleic acid cells, Fm_{470} – maximum fluorescence at 470 nm, Fv/Fm_{470} – maximum photochemical efficiency of PSII measured at 470 nm, $\sigma_{PSII-470}$ – functional absorption

cross-section of PSII measured at 470 nm. Significant difference in means is shown with *** for $p<0.001$, ** for $p<0.01$ and * for $p<0.1$ (two-sample t-test).

[a]Total cells: *Prochlorococcus*+*Synechococcus*+Photosynthetic picoeukaryotes+HNA+LNA cells

[b]Fe limit of detection (LOD) was 0.058 nmol L^{-1}.

Table 2. Relative abundance and characteristics of *Prochlorococcus* and *Synechococcus* oligotypes at two experimental sites at the start of the incubation. The abundance is based on 16S rRNA gene copies and shown as percent of total 16S rRNA gene copies for each genus. Only oligotypes that contributed at least 1% to *Prochlorococcus* and *Synechococcus* populations at both sites are shown. Identity (%) shows percent nucleotide identity to the 16S rRNA gene of the closest strain(s). Score (bits) shows BLASTN score results. eStrain is a representative of a group of strains with 100% identical 16S rRNA gene V3-V4 region.

Oligotype ID	Nucleotides at high entropy positions	Nucleotide identity, %	eStrain	Clade	Relative abundance at GY, %	Relative abundance at TZ, %
Prochlorococcus						
MED4-oligo1	CGTTTCT	100	MED4	HLI	0.96	73.75
MIT9301-oligo1	TGCTAAT	100	MIT9301	HLII	66.19	0.29
MIT9312-oligo1	TACTAAT	100	MIT9312	HLII	21.64	0.45
MIT9515-oligo1	CGCTTCT	100	MIT9515	HLI	0.54	10.72
MED4-oligo2	CGTTTTT	99.75	MED4	HLI	0.55	3.75
MED4-oligo3	CGTTTAT	99.75	MED4	HLI	0.37	2.92
MIT9515-oligo2	CGCTTAT	99.75	MIT9515	HLI	0.64	1.42
SB-oligo1	TGTTAAT	100	SB	HLII	1.93	0.03
MIT9301-oligo2	TGCTTAT	99.51	MIT9301	HLII	1.91	0.04
NATL1A-oligo1	CGCTTTT	99.75	NATL1A	LLI	0.28	1.61
PAC1-oligo1	TGCTTTT	99.75	PAC1	LLI	0.85	0.76
MIT9312-oligo2	TACTTAT	99.51	MIT9312	HLII	1.26	0.01
Synechococcus						
CC9605-oligo1	ATACTCTATGC	100.00	CC9605	Clade II	61.12	34.93
CC9605-oligo2	ATACTCTATGT	99.75	CC9605	Clade II	25.46	14.09
CC9902-oligo1	ATACTCTAAGC	100.00	CC9902	Clade IV	0.00	26.30
CC9902-oligo2	ATACTCTAAGT	99.75	CC9902	Clade IV	0.00	13.64
KORDI100-oligo1	ATCCGCTCTGC	99.75	KORDI-100	Clade V	0.97	5.11
CC9605-oligo3	ATGCTCTATGC	99.75	CC9605	Clade II	5.77	0.00
CC9605-oligo4	ACACTCTATGC	99.75	CC9605	Clade II	4.34	0.34
CC9605-oligo5	ATACTCTCTGC	99.75	CC9605	Clade II	0.48	0.84
KORDI100-oligo2	ATCCGTTCTGT	99.26	KORDI-100	Clade V	0.00	1.10

Table 3. Responses of microbial communities to urea, NO_3^-, NH_4^+ and Fe additions in the North Pacific Ocean. The responses after 48 hrs are summarized for all N forms and specifically for each N substrate. Responses shared between the two stations are shown in grey, and responses specific for TZ and GY stations are shown in orange and blue, respectively. The arrow up (⇑) shows an increase, and the arrow down (⇓) shows a decrease in value. Triangle (Δ) shows a shift in community composition. Reverse triangle (∇) shows consumption of a nutrient (Table S5). The width of arrows and size of triangles reflect the magnitude of change. The empty boxes for individual substrates/elements indicate that the response was similar to that shown in column "All N substrates". The empty boxes in the "All N substrates" indicate that the response differed among all N substrates.

Category	Measurement	All N substrates	Urea	NO_3^-	NH_4^+	Fe
Functional	Chl *a* concentrations					
	^{14}C-PP rates					
	Fm					
	Fv/Fm					
	σ_{PSII}					
Taxonomic I: cell count	*Prochlorococcus*					
	Synechococcus					
	PPE					
	HNA cells					
Taxonomic II: community composition based on 16S rRNA gene	Heterotrophic microbial community					
	Prochlorococcus					
	Synechococcus					
Nutrient consumption	N substrate					
	PO_4^{3-}					

Differential effects of nitrate, ammonium and urea as N sources for microbial communities in the North Pacific Ocean

Authors

[1]Shilova IN[a], [2]Mills MM[a], [3]Robidart JC, [1]Turk-Kubo KA, [4]Björkman KM, [1]Kolber Z, [5]Rapp I., [2]van Dijken GL, [4]Church MJ[†], [2]Arrigo KR, [5]Achterberg EP, [1]Zehr JP*

Figures

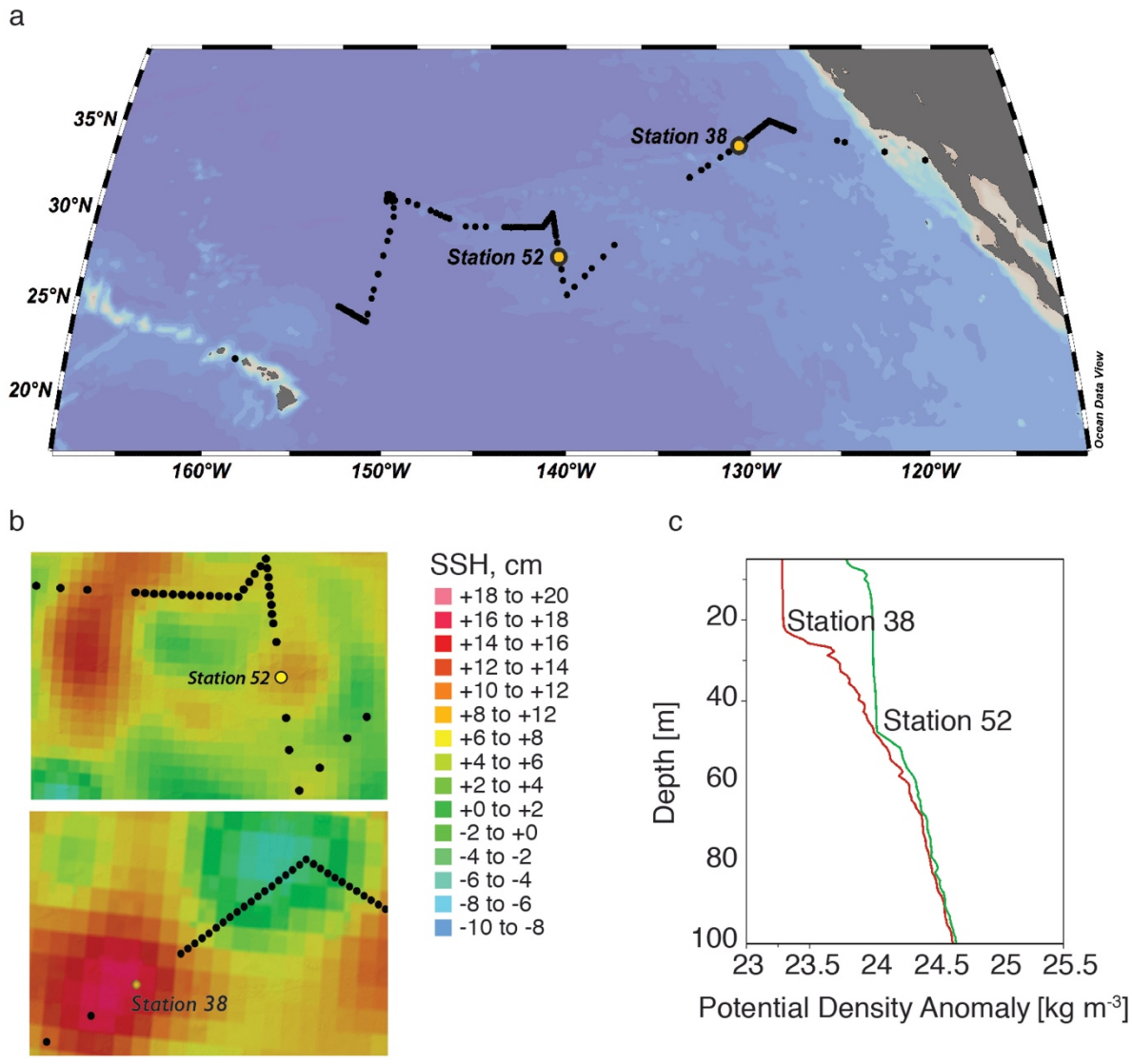

Figure 1

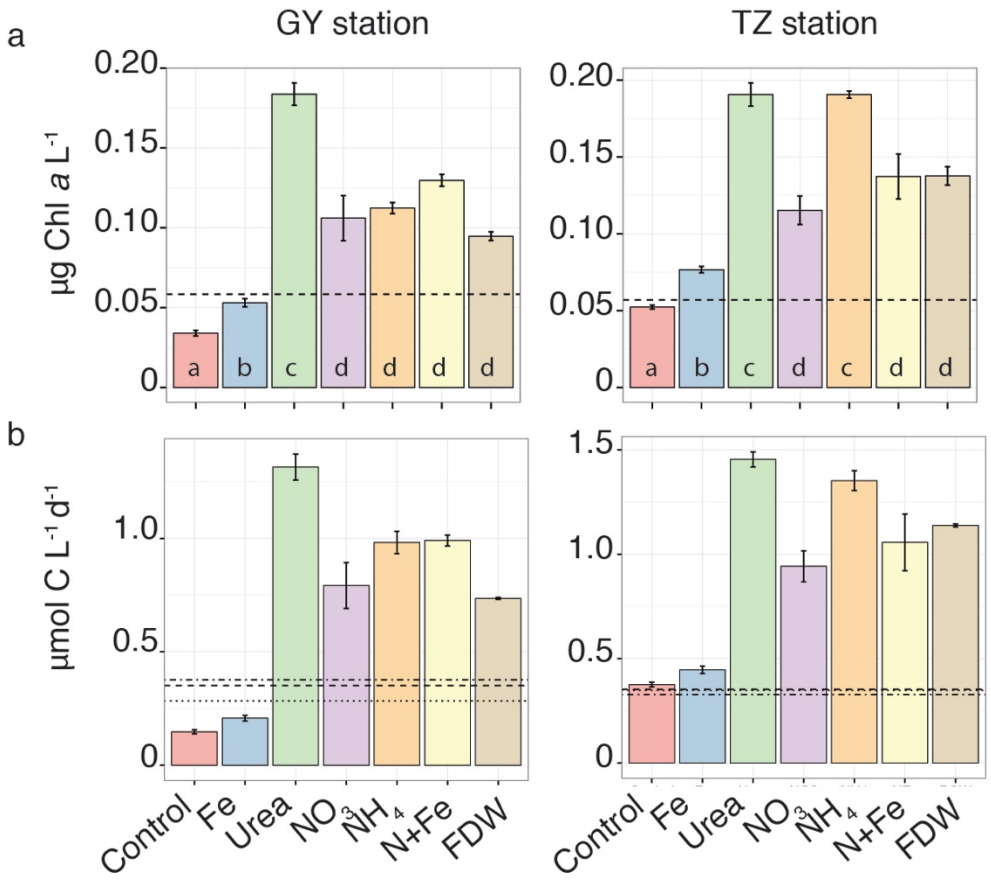
a
GY station
TZ station
µg Chl a L-1
0.20
0.15
0.10
0.05
0
a
b
c
d
d
d
d
a
b
c
d
c
d
d
b
µmol C L-1 d-1
1.5
1.0
0.5
0
Control
Fe
Urea
NO3
NH4
N+Fe
FDW

Figure 2

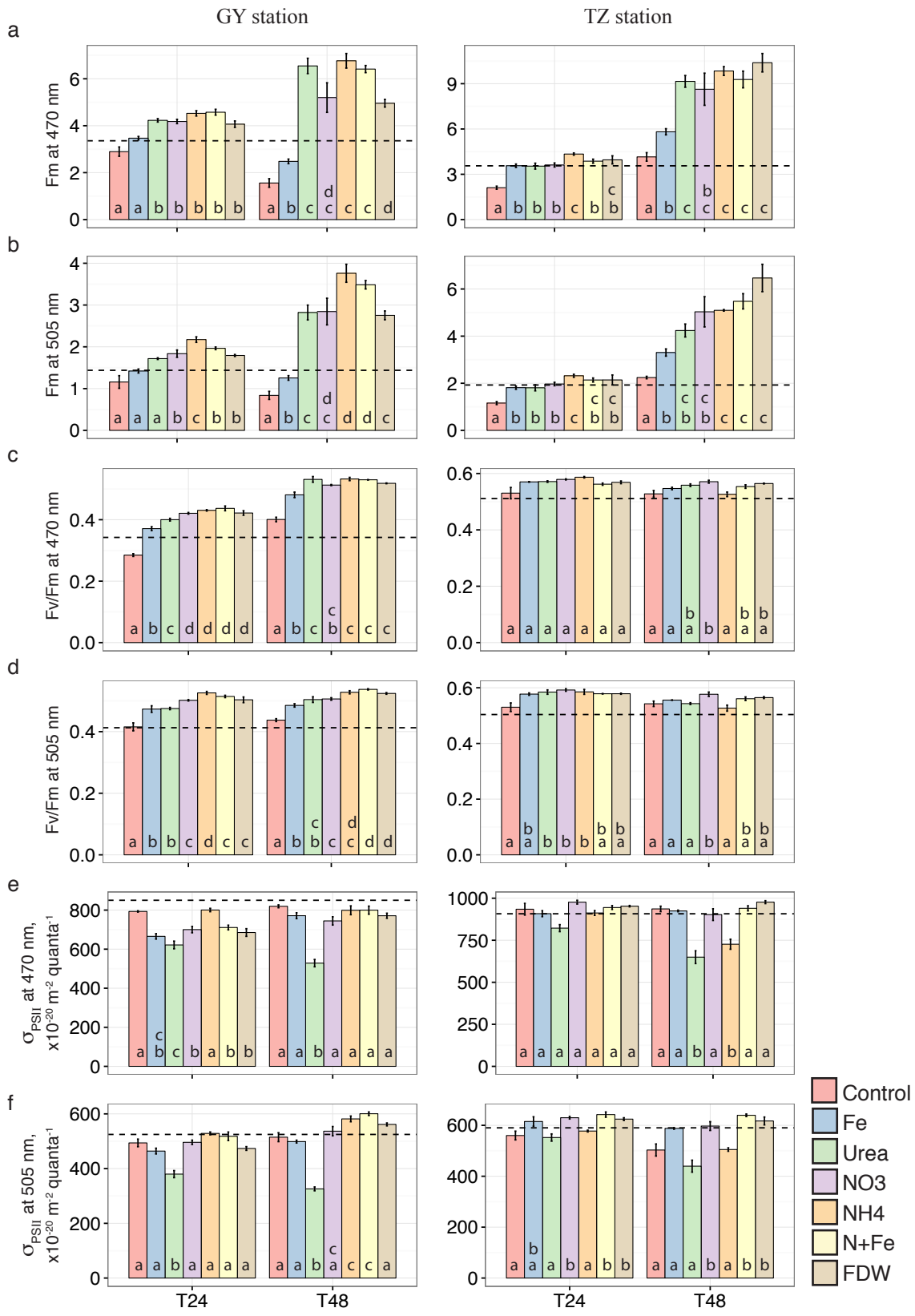
GY station
TZ station
a
b
c
d
e
f
Fm at 470 nm
Fm at 505 nm
Fv/Fm at 470 nm
Fv/Fm at 505 nm
σPSII at 470 nm, x10-20 m-2 quanta-1
σPSII at 505 nm, x10-20 m-2 quanta-1
T24
T48
Control
Fe
Urea
NO3
NH4
N+Fe
FDW

Figure 3

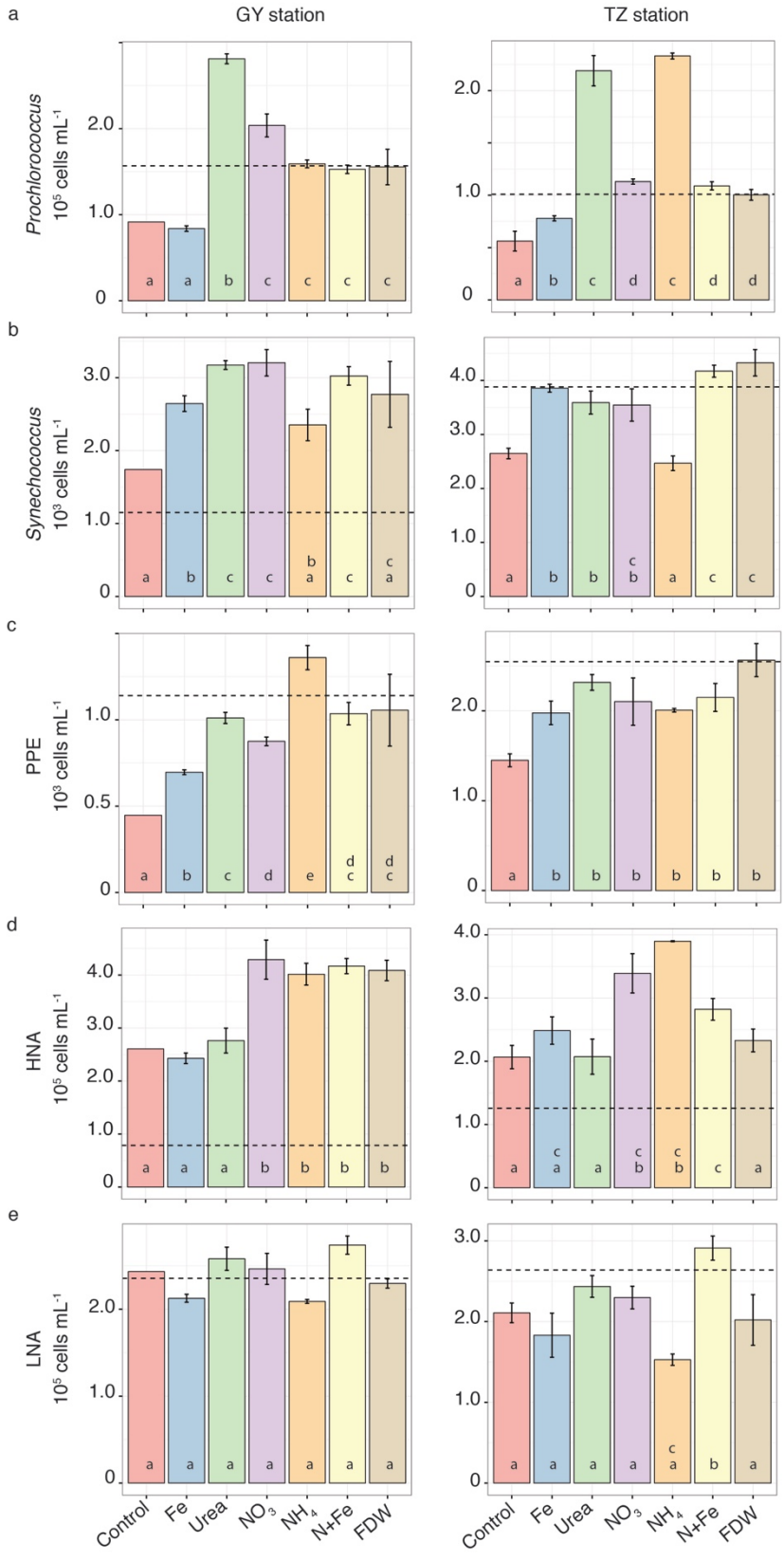
a
GY station
TZ station
Prochlorococcus
10⁵ cells mL⁻¹
b
Synechococcus
10³ cells mL⁻¹
c
PPE
10³ cells mL⁻¹
d
HNA
10⁵ cells mL⁻¹
e
LNA
10⁵ cells mL⁻¹
Control
Fe
Urea
NO3
NH4
N+Fe
FDW

Figure 4

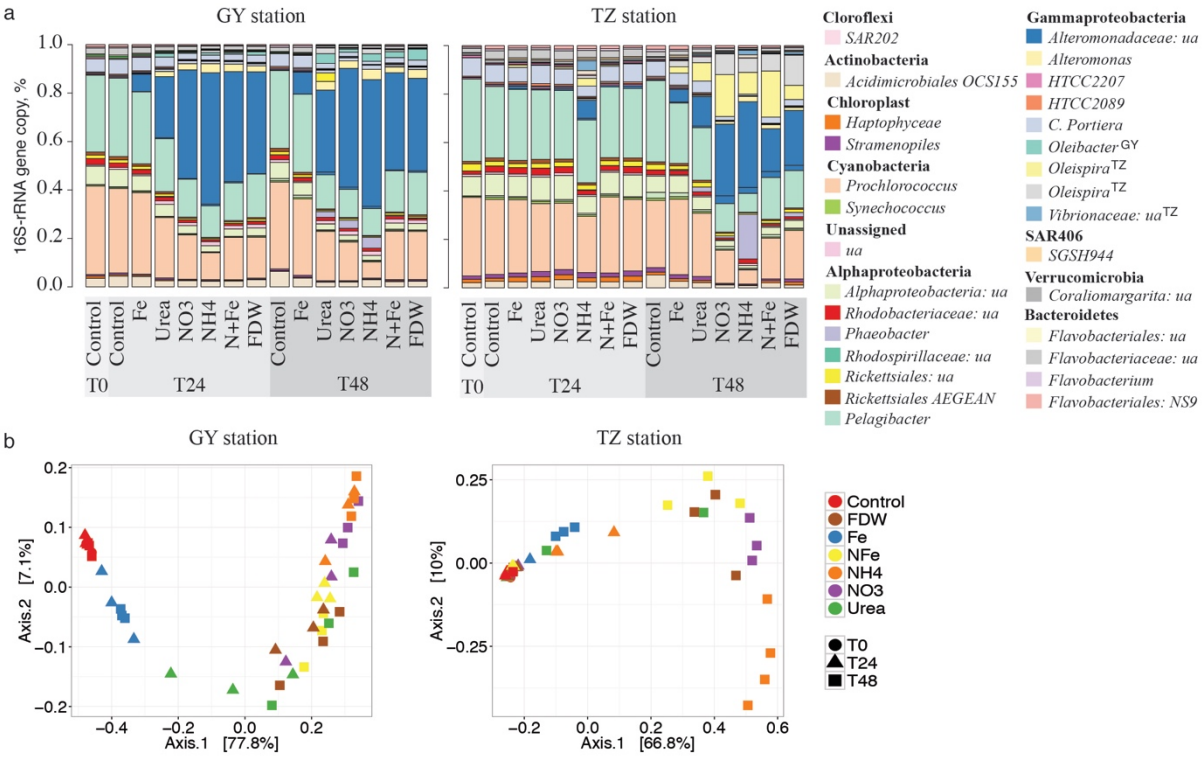
a
GY station
TZ station
16S-rRNA gene copy, %
1.0
0.8
0.6
0.4
0.2
0.0
Control
Control
Fe
Urea
NO3
NH4
N+Fe
FDW
T0
T24
T48
Cloroflexi
SAR202
Actinobacteria
Acidimicrobiales OCS155
Chloroplast
Haptophyceae
Stramenopiles
Cyanobacteria
Prochlorococcus
Synechococcus
Unassigned
ua
Alphaproteobacteria
Alphaproteobacteria: ua
Rhodobacteriaceae: ua
Phaeobacter
Rhodospirillaceae: ua
Rickettsiales: ua
Rickettsiales AEGEAN
Pelagibacter
Gammaproteobacteria
Alteromonadaceae: ua
Alteromonas
HTCC2207
HTCC2089
C. Portiera
Oleibacter GY
Oleispira TZ
Oleispira TZ
Vibrionaceae: ua TZ
SAR406
SGSH944
Verrucomicrobia
Coraliomargarita: ua
Bacteroidetes
Flavobacteriales: ua
Flavobacteriaceae: ua
Flavobacterium
Flavobacteriales: NS9
b
GY station
TZ station
Axis.2 [7.1%]
Axis.1 [77.8%]
Axis.2 [10%]
Axis.1 [66.8%]
Control
FDW
Fe
NFe
NH4
NO3
Urea
T0
T24
T48

Figure 5

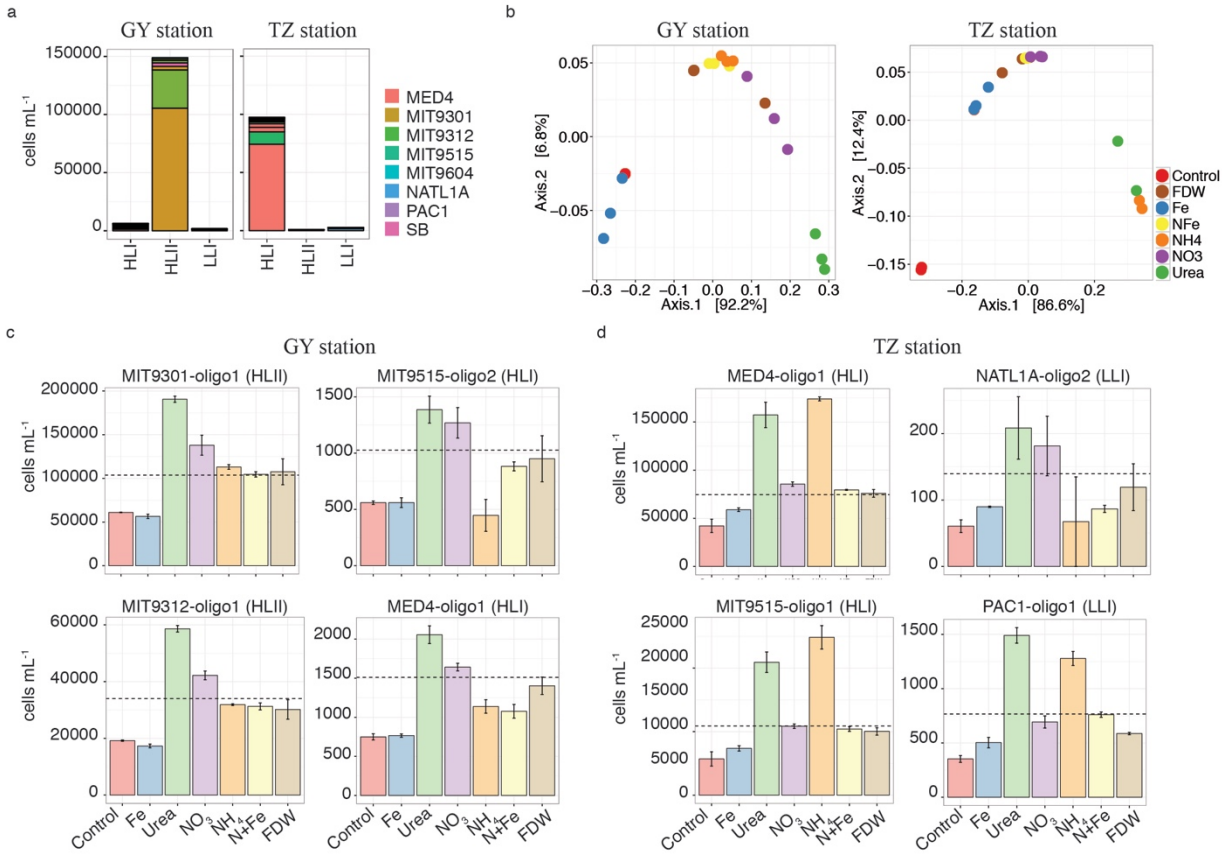
a
GY station
TZ station
cells mL⁻¹
150000
100000
50000
0
HLI
HLII
LLI
MED4
MIT9301
MIT9312
MIT9515
MIT9604
NATL1A
PAC1
SB
b
GY station
TZ station
Axis.2 [6.8%]
Axis.1 [92.2%]
Axis.2 [12.4%]
Axis.1 [86.6%]
Control
FDW
Fe
NFe
NH4
NO3
Urea
c
GY station
MIT9301-oligo1 (HLII)
MIT9515-oligo2 (HLI)
MIT9312-oligo1 (HLII)
MED4-oligo1 (HLI)
d
TZ station
MED4-oligo1 (HLI)
NATL1A-oligo2 (LLI)
MIT9515-oligo1 (HLI)
PAC1-oligo1 (LLI)
Control
Fe
Urea
NO3
NH4
N+Fe
FDW

Figure 6

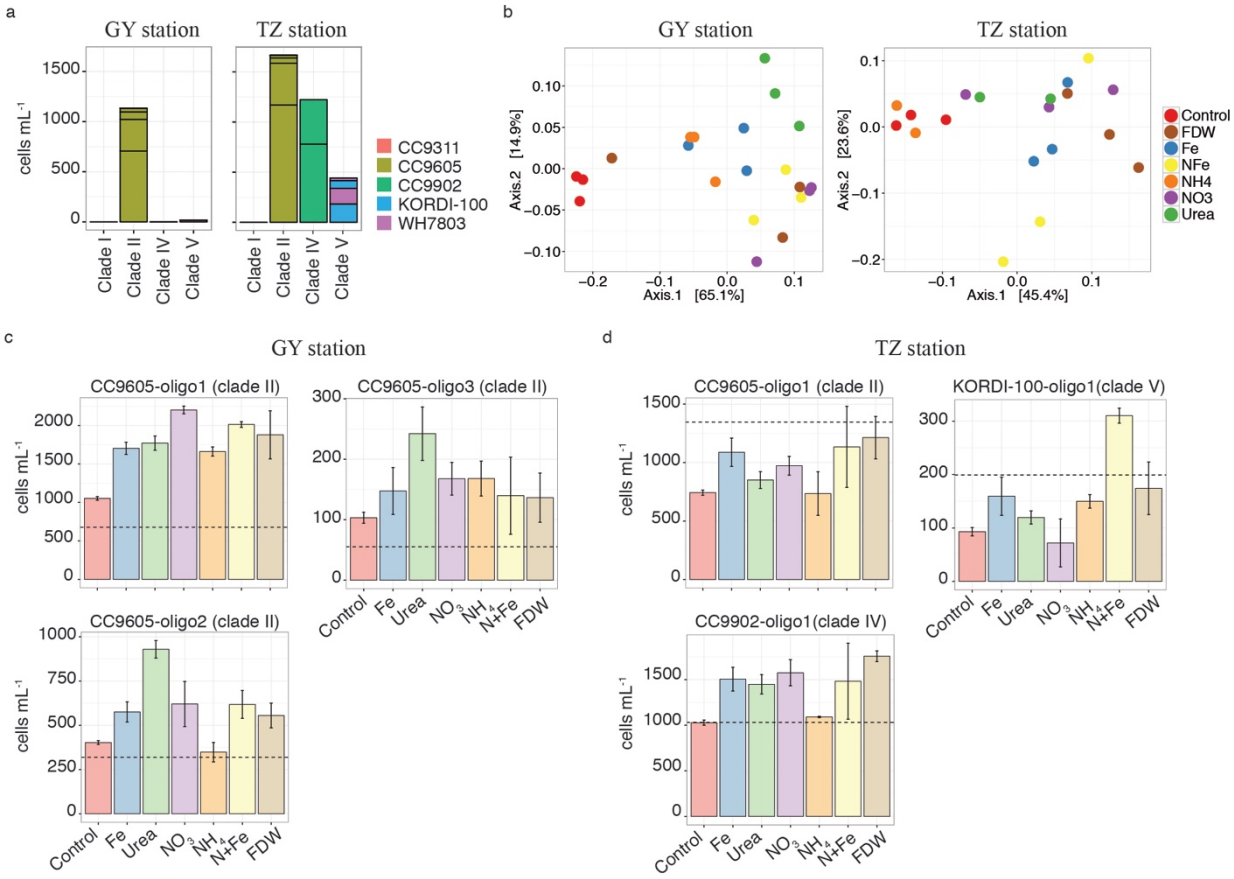
a
GY station
TZ station
cells mL-1
Clade I
Clade II
Clade IV
Clade V
CC9311
CC9605
CC9902
KORDI-100
WH7803
b
GY station
TZ station
Axis.2 [14.9%]
Axis.1 [65.1%]
Axis.2 [23.6%]
Axis.1 [45.4%]
Control
FDW
Fe
NFe
NH4
NO3
Urea
c
GY station
CC9605-oligo1 (clade II)
CC9605-oligo3 (clade II)
CC9605-oligo2 (clade II)
d
TZ station
CC9605-oligo1 (clade II)
KORDI-100-oligo1(clade V)
CC9902-oligo1(clade IV)
Control
Fe
Urea
NO3
NH4
N+Fe
FDW

Figure 7

Title

Differential effects of nitrate, ammonium and urea as N sources for microbial communities in the North Pacific Ocean

Authors

[1]Shilova IN[a], [2]Mills MM[a], [3]Robidart JC, [1]Turk-Kubo KA, [4]Björkman KM, [1]Kolber Z, [5]Rapp I., [2]van Dijken GL, [4]Church MJ, [2]Arrigo KR, [5]Achterberg EP, [1]Zehr JP*

Supplementary Information

Table S1. Oligotypes annotation: strains with identical nucleotide sequence in the V3-V4 region of the 16S-rRNA gene were grouped into eStrains.

Organism	eStrain	Strains
Prochlorococcus	MED4	*Prochlorococcus marinus* str. EQPAC1
		Prochlorococcus marinus MED4
	MIT9301	*Prochlorococcus marinus* str. GP2
		Prochlorococcus marinus str. MIT 9401
		Prochlorococcus marinus str. MIT 9322
		Prochlorococcus marinus str. MIT 9321
		Prochlorococcus marinus str. MIT 9314
		Prochlorococcus sp. MIT 0604
		Prochlorococcus marinus str. MIT 9202
		Prochlorococcus marinus str. MIT 9215
		Prochlorococcus marinus str. MIT 9301
		Prochlorococcus marinus str. AS9601
	MIT9312	*Prochlorococcus marinus* str. MIT 9311
		Prochlorococcus marinus str. PAC1
		Prochlorococcus marinus str. MIT 9302
		Prochlorococcus marinus str. MIT 9107
		Prochlorococcus marinus str. MIT 9123
		Prochlorococcus marinus str. MIT 9201
		Prochlorococcus marinus str. MIT 9116
		Prochlorococcus marinus str. MIT 9312
	MIT9515	*Prochlorococcus marinus* str. MIT 9515
	NATL1A	*Prochlorococcus* sp. MIT 0801
		Prochlorococcus marinus str. NATL1A
		Prochlorococcus marinus str. MIT 9515
	PAC1	*Prochlorococcus marinus* str. PAC1
	SB	*Prochlorococcus marinus* str. SB
Synechococcus	CC9311	*Synechococcus* sp. WH 8020
		Synechococcus sp. CC9311
	CC9605	*Synechococcus* sp. WH 8016
		Synechococcus sp. WH 8109
		Synechococcus sp. KORDI-52
		Synechococcus sp. WH 8103
		Synechococcus sp. CC9605
	CC9902	*Synechococcus* sp. BL107
		Synechococcus sp. CC9902
	KORDI-100	*Synechococcus* sp. KORDI-100
		Synechococcus sp. CC9616

Table S2. T-test statistics summary for evaluating means for chlorophyll *a* concentrations and rates of primary productivity.

Table S3. T-test statistics summary for evaluating means for FRRF parameters: Fm, Fv/Fm and σ_{PSII}.

Table S4. T-test statistics summary for evaluating means for phytoplankton and bacterial group cell counts.

Table S5. Nutrient consumption at the end of the experiments (concentrations at T0 – concentrations at T48). Percentage of nutrient utilized is shown in parenthesis. Urea concentrations were not measured.

Experiment	Treatment	N+N nmol L^{-1}	NH_4^+ nmol L^{-1}	SRP nmol L^{-1}
TZ	NH4		2400±180 (48)	62±8 (23)
	NO3	1480±64 (30)		33±8 (12)
	Urea*			34±9 (13)
	NFe	470±100 (17)	5300±140 (99)	
GY	NH4		1360±92 (54)	27±7 (29)
	NO3	1040±240 (41)		36±8 (38)
	Urea*			36±15 (38)
	NFe	620±160 (28)	2040±60 (97)	33±7 (37)

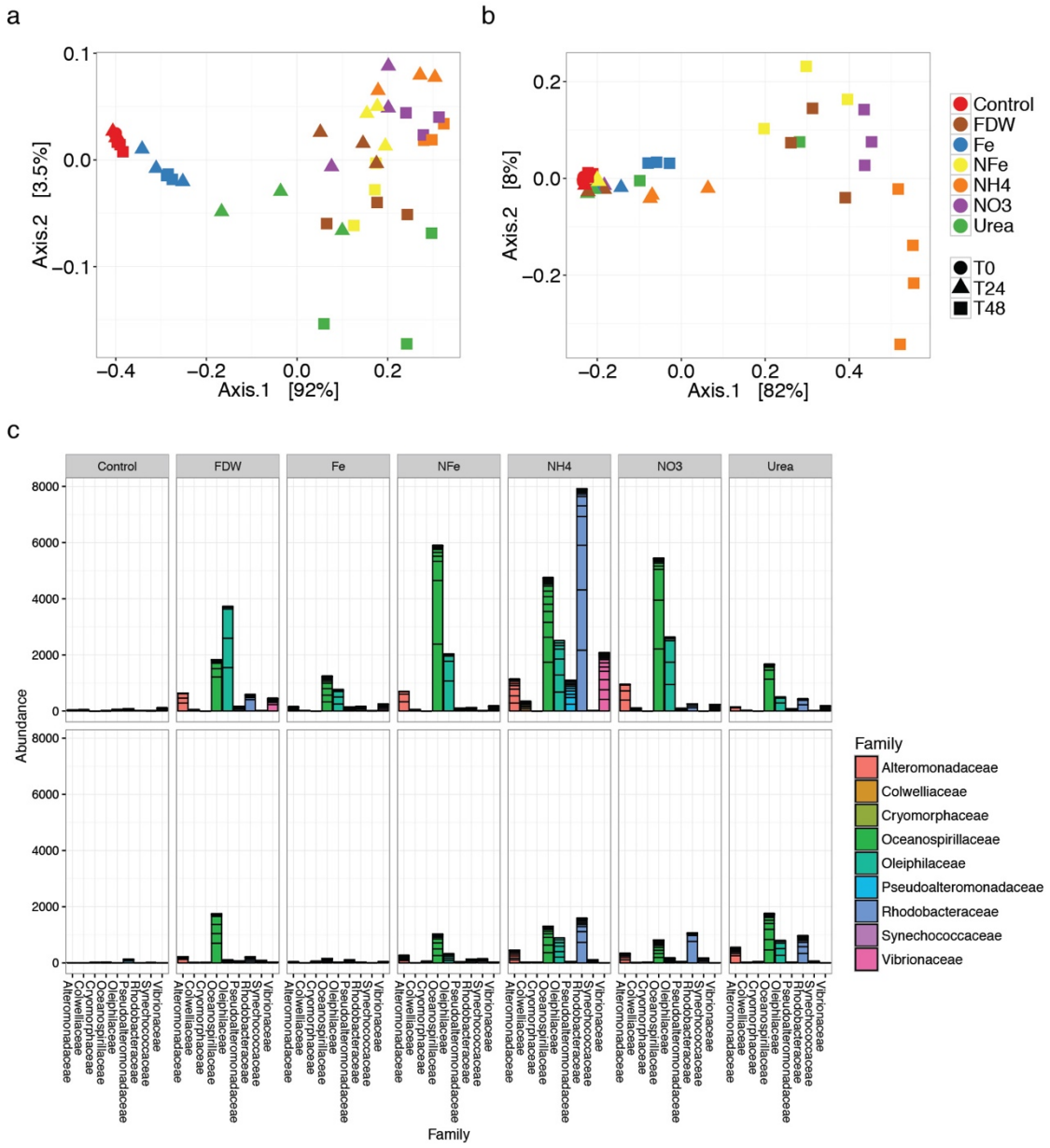

Figure S1. PCoA of heterotrophic community composition shifts in response to nutrient addition measured with the Bray-Curtis index produced similar results to the PCoA based on the Jaccard index (as shown in Fig. 5). (a) GY station, and (b) TZ station. The samples are color-coded by treatment and the shape corresponds to the time of sampling. (c) Relative abundances of 16S-rRNA sequences for most variable microbial families shown for the TZ (top panel) and GY stations (bottom panel).

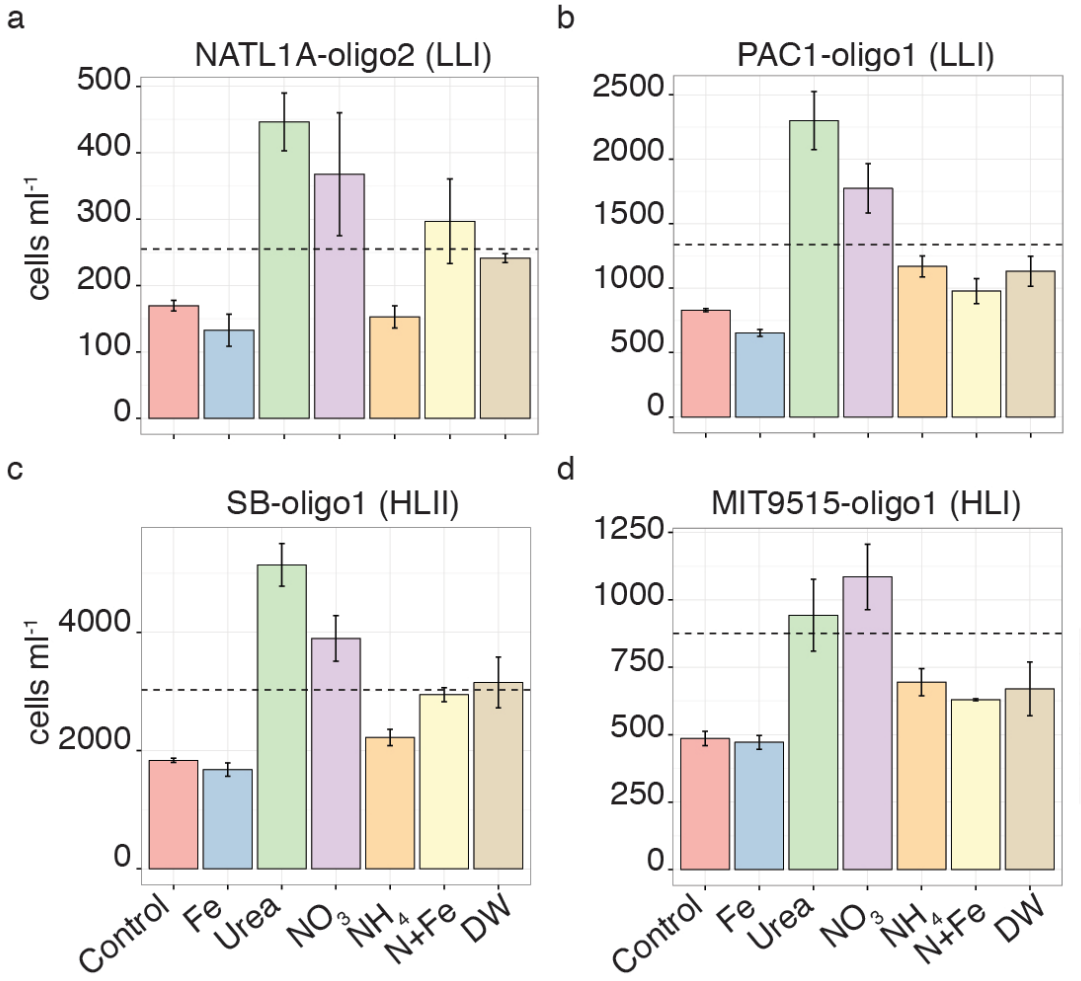

Figure S2. Differential responses of *Prochlorococcus* oligotypes to N compounds. Cell abundances of the selected *Prochlorococcus* oligotypes in response to nutrient additions after 48 of incubation at the GY station. The dashed line shows cell abundances of each oligotype at T0.